AD-A084 737 COLD REGIONS RESEARCH AND ENGINEERING LAB HANOVER NH F/G 8/12
MATHEMATICAL MODEL TO CORRELATE FROST HEAVE OF PAVEMENTS WITH L--ETC(U)
FEB 80 R L BERG, G L GUYMON, T C JOHNSON
UNCLASSIFIED CRREL-80-10 NL

1 OF 1
AD
AD-A084 737

END
DATE FILMED
7-80
DTIC

CRREL

REPORT 80-13

Mathematical model to correlate frost heave of pavements with laboratory predictions

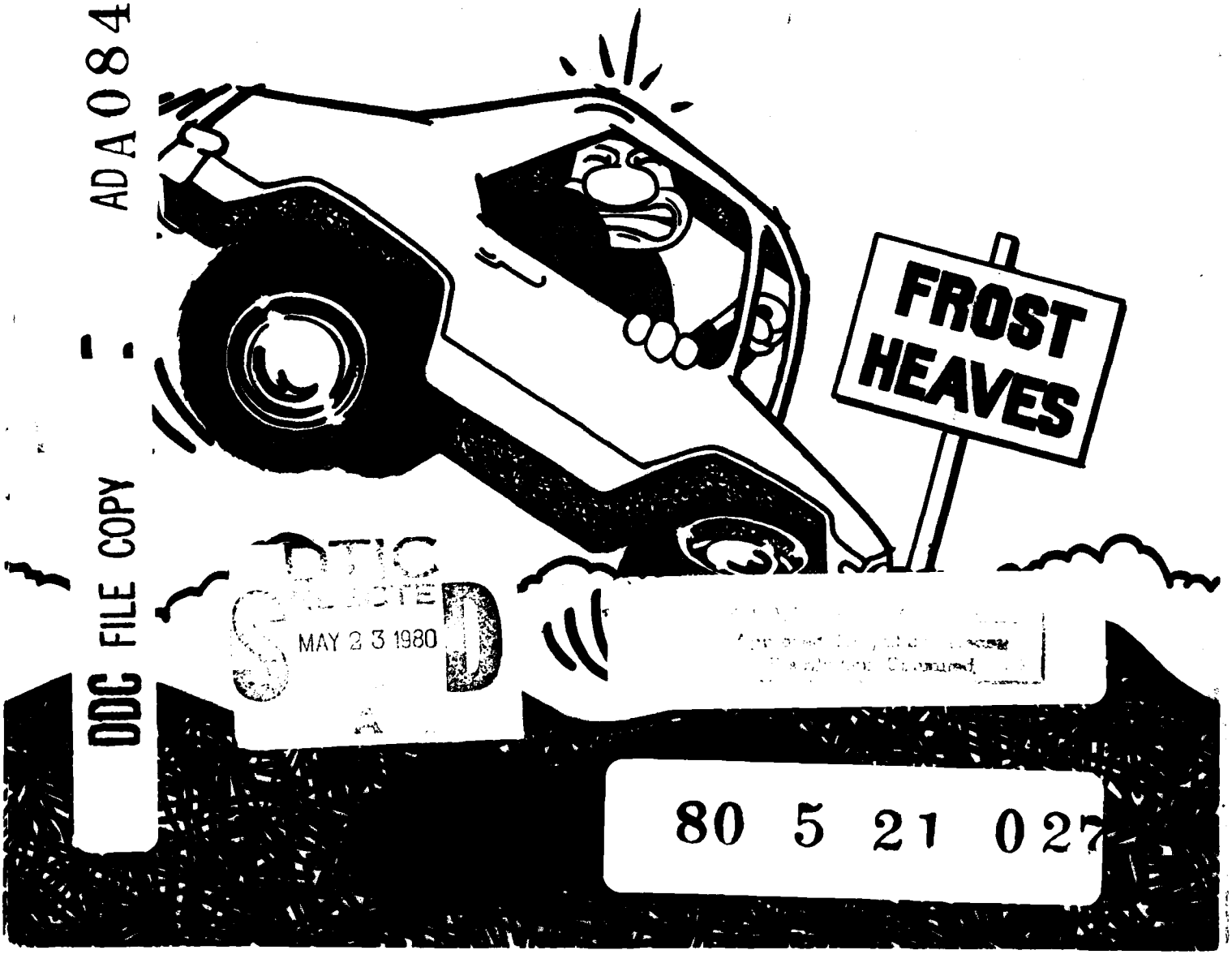

For conversion of SI metric units to U.S./British customary units of measurement consult ASTM Standard E380, Metric Practice Guide, *published by the American Society for Testing and Materials, 1916 Race St., Philadelphia, Pa. 19103.*

CRREL Report 80-10

Mathematical model to correlate frost heave of pavements with laboratory predictions

R.L. Berg, G.L. Guymon and T.C. Johnson

February 1980

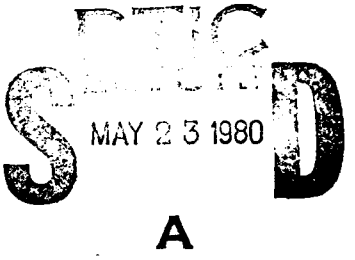

Prepared for
FEDERAL HIGHWAY ADMINISTRATION
OFFICE OF RESEARCH
By
UNITED STATES ARMY
CORPS OF ENGINEERS
COLD REGIONS RESEARCH AND ENGINEERING LABORATORY
HANOVER, NEW HAMPSHIRE, U.S.A.

Unclassified

SECURITY CLASSIFICATION OF THIS PAGE (When Data Entered)

REPORT DOCUMENTATION PAGE

READ INSTRUCTIONS BEFORE COMPLETING FORM

1. REPORT NUMBER: CRREL Report 80-10	2. GOVT ACCESSION NO.: AD-A084 737
3. RECIPIENT'S CATALOG NUMBER	
4. TITLE (and Subtitle): MATHEMATICAL MODEL TO CORRELATE FROST HEAVE OF PAVEMENTS WITH LABORATORY PREDICTIONS	5. TYPE OF REPORT & PERIOD COVERED
	6. PERFORMING ORG. REPORT NUMBER
7. AUTHOR(s): R.L. Berg, G.L. Guymon and T.C. Johnson	8. CONTRACT OR GRANT NUMBER(s): Intra-Government Order 5-3-0202
9. PERFORMING ORGANIZATION NAME AND ADDRESS: U.S. Army Cold Regions Research and Engineering Laboratory, Hanover, New Hampshire 03755	10. PROGRAM ELEMENT, PROJECT, TASK AREA & WORK UNIT NUMBERS: DA Project 4A762730AT42, Task D, Work Unit 004
11. CONTROLLING OFFICE NAME AND ADDRESS: Federal Highway Administration, Office of Research, Washington, D.C. 20590	12. REPORT DATE: February 1980
	13. NUMBER OF PAGES: 54
14. MONITORING AGENCY NAME & ADDRESS (if different from Controlling Office)	15. SECURITY CLASS. (of this report): Unclassified
	15a. DECLASSIFICATION/DOWNGRADING SCHEDULE

16. DISTRIBUTION STATEMENT (of this Report)

Approved for public release; distribution unlimited.

17. DISTRIBUTION STATEMENT (of the abstract entered in Block 20, if different from Report)

18. SUPPLEMENTARY NOTES

Partially funded by the U.S. Army Corps of Engineers and the Federal Aviation Administration.

19. KEY WORDS (Continue on reverse side if necessary and identify by block number)

Computerized simulation
Soil tests
Frost heave
Laboratory tests
Mathematical models
Pavements

20. ABSTRACT (Continue on reverse side if necessary and identify by block number)

A mathematical model of coupled heat and moisture flow in soils has been developed. The model includes algorithms for phase change of soil moisture and frost heave and permits several types of boundary and initial conditions. The finite element method of weighted residuals (Galerkin procedure) was chosen to simulate the spatial regime and the Crank-Nicholson method was used for the time domain portion of the model. To facilitate evaluation of the model, the heat and moisture fluxes were essentially decoupled; moisture flux was then simulated accurately, as were heat flux and frost heave in a laboratory test. Comparison of the simulated and experimental data illustrates the importance of unsaturated hydraulic conductivity. It is one parameter which is difficult to measure and for which only a few laboratory test results are available. Therefore, unsaturated hydraulic conductivities calculated in the computer model

DD FORM 1 JAN 73 1473 EDITION OF 1 NOV 65 IS OBSOLETE

Unclassified

SECURITY CLASSIFICATION OF THIS PAGE (When Data Entered)

20. Abstract (cont'd).

may be a significant source of error in calculations of frost heave. The algorithm incorporating effects of surcharge and overburden was inconclusively evaluated. Time-dependent frost penetration and frost heave in laboratory specimens were closely simulated with the model. After 10 days of simulation, the computed frost heave was about 2.3 cm vs 2.0 cm and 2.8 cm in two tests. Frost penetration was computed as 15 cm and was measured at 12.0 cm and 12.2 cm in the two laboratory samples after 10 days.

PREFACE

This report was prepared by Dr. R.L. Berg, Research Civil Engineer, Geotechnical Research Branch, Experimental Engineering Division, U.S. Army Cold Regions Research and Engineering Laboratory, Dr. G.L. Guymon, Chairman of Civil Engineering, University of California at Irvine, and T.C. Johnson, Civil Engineer, Civil Engineering Research Branch, Experimental Engineering Division, CRREL.

The study was jointly funded by the Federal Highway Administration (FHWA), the U.S. Army Corps of Engineers, and the Federal Aviation Administration (FAA) under Intra-Government Order 5-3-0202.

A. Di Millio of the Federal Highway Administration and S. Connistra of the Federal Aviation Administration technically reviewed the manuscript of this report.

Special recognition is given to J.E. Ingersoll who conducted or supervised most of the laboratory studies and to K.L. Gartner, M. Morton and T. Hromadka for accomplishing much of the computer programming. Capt. Cameron Appel, now deceased, worked a relatively short time on this study, but contributed greatly to its accomplishment.

It must be emphasized that this report represents results completed through early 1979. Research in frost heave modeling is progressing at a rapid rate and new refinements and additional results are being continuously completed. This report therefore should be considered as describing the state-of-the-art when it was written.

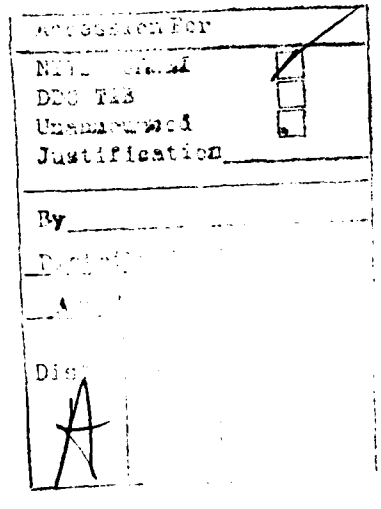

CONTENTS

ILLUSTRATIONS

TABLES

MATHEMATICAL MODEL TO CORRELATE FROST HEAVE OF PAVEMENTS WITH LABORATORY PREDICTIONS

R.L. Berg, G.L. Guymon and T.C. Johnson

INTRODUCTION

Taber (1930) stated, "Freezing and thawing have caused much damage to road pavements in cold climates, but the processes involved have not been clearly understood, and therefore some of the preventive measures adopted have proved to be of little or no value."

Taber's comment is still true today. Although federal, state and local governments have spent huge amounts of money to repair frost damaged road and airfield pavements and have made significant expenditures on the development of tests to determine the "frost susceptibility" of soils, relatively little effort has been expended to develop a more complete understanding of the physics, chemistry and mechanics of the frost heaving process. During the development of the mathematical model to describe the frost heaving process that is discussed in this report, we learned that significant scientific advances must still be made. Many of these problem areas will be discussed in subsequent sections of this report.

Within pavement systems, frost action is manifested by heaving of the surface during freezing and/or a decrease in the load carrying capacity of the pavement during thawing. On roads severely affected by frost heave, vehicle running speeds must be sharply reduced to avoid loss of vehicle control on the rough pavement. At airfields which have severe differential frost heave problems, it may be necessary to close all or a portion of a runway to aircraft traffic.

Conversely, some pavements cannot support the design loads during "thaw weakened" periods, and where reduced loads are not imposed the deterioration rates of these underdesigned pavements are dramatically increased. At some airfields it is necessary to restrict the type or weight of aircraft which may operate on certain pavement features during spring thaw. At the same time, a number of states impose load restrictions on some highway pavements during the spring when thawing occurs.

The following discussion, contained in the prospectus for this study, is presented here to summarize the basis for this study. Several points in the discussion are amplified in subsequent sections of this report.

Techniques to eliminate frost associated problems by means of thermal insulation or soil modification to prevent moisture transfer have been attempted, but are not being used extensively because they have undesirable side effects, are too expensive or are not universally effective. The most widely applied technique for controlling the detrimental effects of frost action is to place non-frost-susceptible base or subbase material to a depth equal to some fraction of the anticipated frost penetration. The availability of high quality (non-frost-susceptible) granular materials has been severely depleted by the construction of the Interstate system. Prudent use should be made of the remaining materials, conserving them for the most essential purposes. To provide frost-resistant pavements new sources of materials must be located, new standards of frost-susceptibility of soils and materials must be adopted, and techniques to beneficiate unacceptable materials developed.

Almost all frost heave susceptibility criteria currently used are based on the particle-size distribution of the soil. Empirical methods and attendant criteria based on particle-size distribution have been widely used because they are relatively simple and rapid. The criteria are not consistently reliable, however, and soils meeting the established criteria may be frost heave susceptible, while other soils not meeting the criteria may actually be non-frost-susceptible. Criteria based on

particle-size distribution are frequently misleading because it is very difficult to apply empirical rules to a very complex phenomenon. Various researchers have identified a number of parameters, other than particle-size distribution, which influence the susceptibility of soil and state of stress in the water; rate of frost penetration, overburden pressure, permeability, soil skeleton (size, shape and distribution of soil pores), cyclic freezing and thawing, and soil density are among those factors that have been identified as influencing the severity of frost heave.

It is unlikely that a consistently reliable method for evaluating or predicting a soil's frost heave susceptibility can be based upon measurement of only one of the above factors, because a number of them are interdependent. A realistic laboratory assessment of a soil's frost heave potential requires a test that reflects the soil's behavior while it is simultaneously subjected to the influence of all these variables. To avoid the shortcomings of empiricism, several test methods based on one or more of the aforementioned factors, which more rationally and rapidly evaluate frost heave potential, have recently been developed. The permeability test and the heave stress test were developed at MIT. The rapid frost heave test was developed at the University of New Hampshire. The appropriate freezing rate test developed by Penner in Canada has also recently been recommended in the literature. Interpretation of early results from the first 1 to 2 days of freezing in the CRREL standard freezing test method provides a relative frost heave susceptibility rating. To date none of the proposed new methods for rating the frost heave potential of a soil enumerated above has been correlated with field performance data. Evaluation of the efficiency of these laboratory tests in categorizing the heave susceptibility of particular soils requires that predicted behavior be compared with observed behavior in the field, where factors not evaluated in any of these laboratory tests, such as cyclic freezing and thawing, may be important.

Research on test equipment is essentially completed for all the test methods mentioned above. More laboratory testing is required to formulate better concepts of the capabilities and limitations of some of the test methods, but correlations of field performance with predictions by these methods should be undertaken immediately.

The original purpose of the research described in this report was to develop a mathematical model to correlate the results obtained from the above laboratory test methods with field performance. As the study progressed it appeared to the project investigators that the mathematical model could probably be used as a design tool to estimate the magnitude of frost heave for various designs and environmental conditions. With further study and refinement, the model may also aid in estimating the degree of thaw weakening and the duration of thaw-weakened conditions.

The two primary objectives of this research were:

1. To develop a mathematical model of frost heave in terms of the significant physical, environmental and climatic factors, and make a sensitivity analysis of the various parameters.

2. To develop a work plan, including staffing and instrumentation requirements, for correlating the results of the various laboratory test methods for assessing frost heave susceptibility of soils and the amount of heave observed in the field, making use of the model developed for this purpose.

The main body of this report addresses the first research objective, i.e. the development of a mathematical model of the frost heaving process. The second objective was accomplished in late 1976 (Berg and Johnson 1976), when an annual report was submitted describing the necessary work. Important sections of that report are contained in Appendix A. Since that work was accomplished, representatives of the three agencies have discussed the requirements for field and laboratory studies on thaw weakening of pavement systems in seasonal frost areas as well as frost heaving of these pavements. The FHWA and FAA originally believed that thaw weakening studies would be conducted subsequent to the frost heave studies. Because most of the instrumentation for field observations on the extent and duration of thaw weakening are the same as those for frost heave-related studies, it was deemed desirable to conduct the tests simultaneously. Appendix B contains a discussion of the laboratory and field studies which should be conducted to evaluate the thaw weakening process.

ONE-DIMENSIONAL EQUATIONS OF SIMULTANEOUS HEAT AND MOISTURE FLUX

Over the last few decades a large number of reports related to heat flux and freezing and thawing in pavement systems have been published (Dempsey 1976). Johnson (1952) lists more than 800 publications on these topics. Dempsey (1969), Christison (1972), and Berg (1976) reference many of the more recent articles pertaining to freezing and thawing effects on pavement systems.

Moisture flux and seasonal changes in moisture contents in pavement systems have not received as much attention as has heat flow in these systems. The two most prominent publications on this topic are *Moisture*

Equilibrium and Moisture Changes in Soils Beneath Covered Areas (Aitchison 1965), the proceedings of a conference held in Australia in 1965, and *Water in Roads: Prediction of Moisture Content of Road Subgrades*, the proceedings of a 1973 meeting held in France by the Organization for Economic Cooperation and Development (OECD 1973). Dempsey (1976) refers to papers from these two meetings as well as several other important publications.

Most literature on coupled heat and moisture flux in soil-water systems has been published in the last decade. Harlan (1972) and Guymon and Luthin (1974) were among the first to apply numerical models to simultaneous heat and moisture flux. An early article by Johnson and Lovell (1953) contained two figures which summarized extrinsic and intrinsic factors affecting frost action in soils. Dempsey (1976) also showed the figures and we again present them as Figures 1 and 2 of this report. Study of these two figures will illustrate the complex relationships which must be considered in developing mathematical models of frost heaving. In the remainder of this section we briefly review the equations of heat and moisture flux in soil-water systems and describe how the equations are coupled. Emphasis is on freezing soil conditions.

The theory and experimental verification of isothermal moisture storage and movement in soils are well advanced (Kirkham and Powers 1972). Likewise, the theory of soil thermal states, dependent on soil moisture storage but independent of soil moisture movement, is well developed (Jumikis 1966, Luikov 1966). It is nevertheless generally recognized that the hydrologic and thermal states of soil systems are coupled, particularly during freezing and thawing processes. In the following discussion a description of the procedure used for coupling the equations of heat and moisture flux is discussed and a numerical analog for their solution is presented.

With adequate computer capability it should be possible to realistically model the complex coupled soil moisture and thermal states of soil systems involving freezing and thawing. The basis for such a model is our current physically based knowledge of component processes combined with phenomenological equations for lumped processes not well understood, and empirically based relationships for parameters arising in the model assumptions. Indeed, with the widespread availability of computers there seems to be little reason for modeling only part of the processes involved (e.g. heat only) when with a little additional effort, more complete models can be developed.

Philip and DeVries (1957) presented a model based on the physics of anisothermal moisture movement in porous media. Nielsen et al. (1972) reviewed the most prominent work relating to anisothermal moisture movement. All of this work is primarily for soil water systems where temperatures are above freezing. More recently, Harlan (1972, 1973) Guymon and Luthin (1974), Jame (1978), and Taylor and Luthin (1978) have developed anisothermal models of soil moisture movement involving freezing and thawing. The key assumption involving the more recent models is that moisture moves in the freezing soil profile predominantly as liquid films and obeys unsaturated flow theory. Harlan (1972, 1973) developed a one-dimensional model and presented a finite difference numerical scheme, as did Taylor and Luthin (1978). Guymon and Luthin (1974) developed a finite element analog for one-dimensional freezing and thawing. Jame (1978) developed a one-dimensional model of a horizontal soil column based on Harlan's work.

Moisture Transport

It is well known that Richards' equation applies to isothermal unsaturated flow in ice-free soil water systems in which the air phase can be neglected. According to Jame and Norum (1972) and Harlan (1973), Richards' equation also applies to systems where ice may be in the soil pores to some certain limiting condition. To elaborate upon this thesis, consider a single pore that is completely filled with water. As temperatures are lowered to the ice nucleation level (i.e. $T < 0°C$), a single crystal of ice commences to form more or less in the center of a pore because of the distribution of free energy in the system (Edlefson and Anderson 1943). If the ice is regarded as an air bubble, a situation analogous to unsaturated flow exists. This view permits the use of unsaturated flow theory where the hydraulic conductivity is changing with respect to liquid moisture content. This view will remain valid up to some limiting condition which will occur when ice in soil pores has developed to the point that Darcy's law no longer applies or interconnected unfrozen water films have been disrupted. This limiting condition, however, is probably at a temperature much lower than that usually encountered in situ.

Our proposed model is based on the following assumptions:

1. Darcy's law applies to moisture movement in both saturated and unsaturated conditions.
2. The porous media are nondeformable as far as moisture flux is concerned. It is well-known, however, that as fine-grained soils freeze, ice lenses form and that the expansion of these lenses together with the expansion of freezing water in pores causes deformations called heaving.

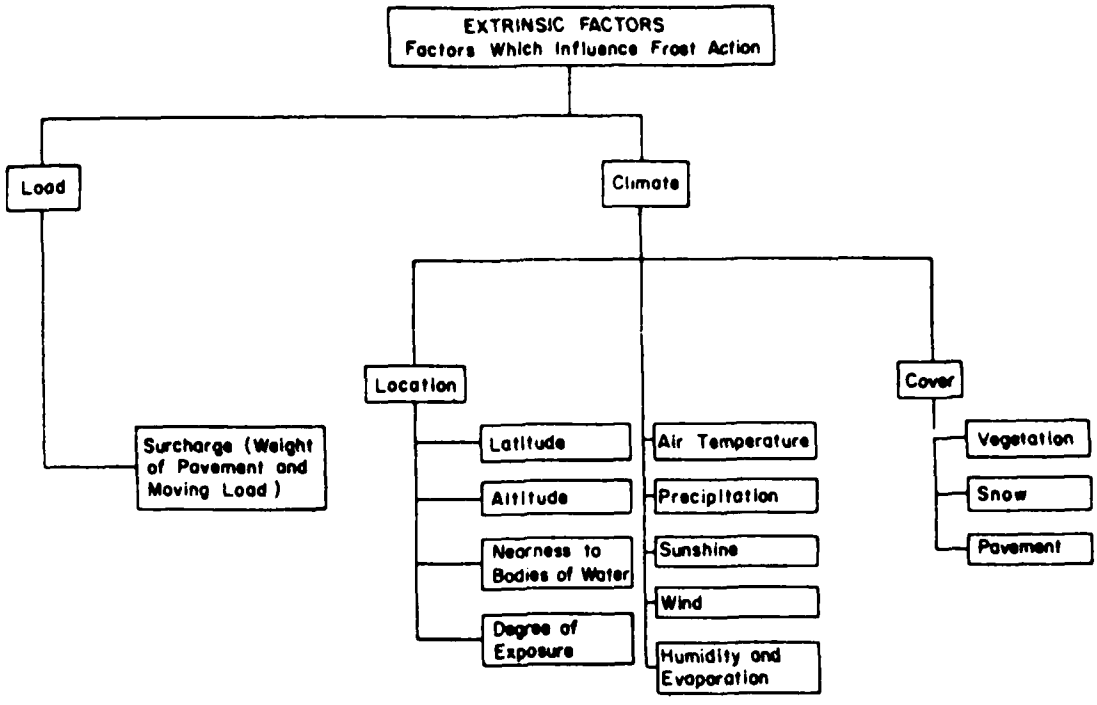

Figure 1. Extrinsic factors influencing frost action (from Johnson and Lovell 1953).

3. All processes are single valued; i.e. hysteresis is not present in relationships such as the soil water characteristic curve.
4. Dissolved salts have a negligible effect on the amount of unfrozen water.
5. Water flux is primarily as liquid; i.e. vapor flux is negligible.

Anisothermal moisture flux in a one-dimensional soil column is governed by Darcy's law plus terms to account for vapor flux and thermally driven moisture and vapor (this flow law may be termed the general Darcy law). Philip and DeVries (1957), Nielsen et al. (1972), and Cary and Mayland (1972) review these relationships. For purposes of this work we assume that the major components of flux are those due to liquid driven by hydraulic gradients. For moist soils, and it is these soils that are of primary interest, vapor transfer driven by thermal and hydraulic gradients and liquid flux driven by thermal gradients are generally several orders of magnitude lower than liquid moisture flux due to hydraulic mechanisms. Since they may contribute a significant convected heat term and may cause heaving, hydraulic mechanisms are the *raison d'etre* for including the moisture state equation in the first place.

A one-dimensional moisture flux relationship is Darcy's law

$$v = -K \frac{\partial \phi}{\partial x} \tag{1}$$

where x = the coordinate axis, positive downward
v = the velocity flux in the x direction, positive downward
ϕ = the total hydraulic head ($\phi = \psi - x$, where ψ is the pore pressure in length units, $\psi < 0$ for unsaturated flow, and $\psi > 0$ for saturated flow)
$K = K(\psi, T)$ the hydraulic conductivity
T = temperature.

Substituting eq 1 into the continuity equation applicable to freezing soils

$$\frac{\partial v}{\partial x} = -\frac{\partial \theta}{\partial t} - Q_1 \tag{2}$$

yields an equation similar to Richards' equation, i.e.

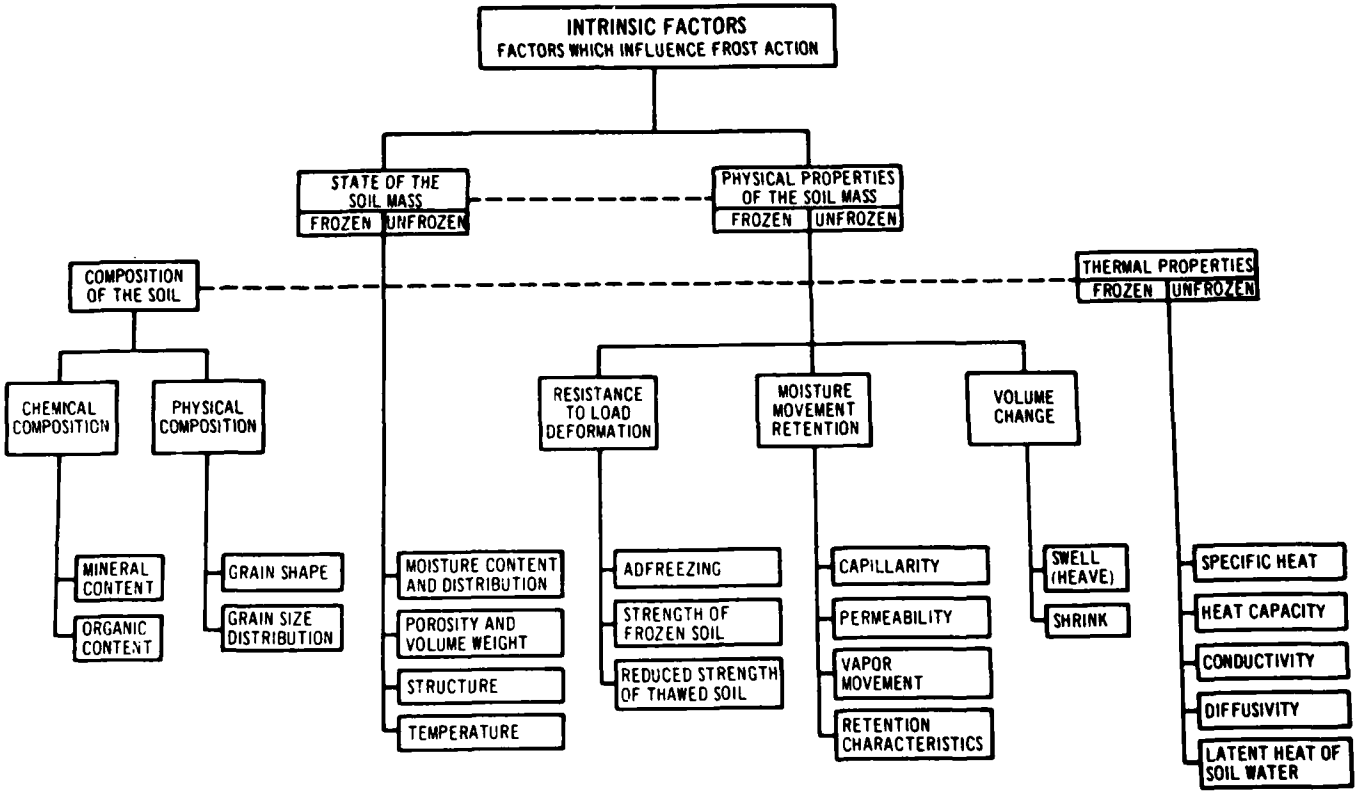

Figure 2. Intrinsic factors influencing frost action (from Johnson and Lovell 1953).

$$\frac{\partial(K\,\partial\psi/\partial x)}{\partial x} - \frac{\partial K}{\partial x} = \frac{\partial\theta}{\partial t} + Q_I \qquad (3)$$

where $\theta = \theta(\psi, T, t,)$, the volumetric liquid water content
Q_I = the rate at which liquid water is converted to ice
t = time.

As eq 3 now stands, it can be solved numerically with approximate boundary conditions; however, suitable approximations are introduced such that the storage and gravitational components of the equation are cast in terms of the state variable ψ which provides for some computational convenience and is required to apply the finite element method. It is assumed that K and θ can be approximated by relationships proposed by Gardner (1958); i.e.

$$K = K_0 \qquad \psi \geq 0$$

$$K = K_0/(-A_k\psi^3+1) \qquad \psi < 0 \qquad (4)$$

$$\theta = \theta_0 \qquad \psi \geq 0$$

$$\theta = \theta_0/(-A_w\psi^3+1) \qquad \psi < 0 \qquad (5)$$

where K_0 and θ_0 are the saturated hydraulic conductivity and saturated volumetric moisture content (porosity), respectively, and A_k and A_w are parameters depending on the soil. Other relationships similar to eq 4 and 5 could be used, e.g. empirically determined equations for particular soils. The Gardner relationships are used because they were the first such relationships to be considered in this research. They also serve to illustrate the mathematical technique used in transforming eq 3 into an equation containing a single state variable. Since K and θ are assumed to be continuous single-valued functions of ψ, this in effect assumes that the soil water system has no "memory." Many soils exhibit hysteresis, which is, in a systems sense, memory of past states of the system. Further, eq 4 and 5 are not functions of the temperature; this will be discussed following further mathematical development.

Taking the partial derivative of eq 4 with respect to x and the partial derivative of eq 5 with respect to t yields

$$\frac{\partial K}{\partial x} = K^* \frac{\partial\psi}{\partial x} \qquad \psi < 0 \qquad (6a)$$

$$\frac{\partial\theta}{\partial t} = \theta^* \frac{\partial\psi}{\partial t} \qquad \psi < 0 \qquad (7a)$$

where

$$K^* = \frac{3A_kK_0\psi^2}{(-A_K\psi^3+1)^2} \qquad (6b)$$

$$\theta^* = \frac{3A_w\theta_0\psi^2}{(-A_w\psi^3+1)^2} \qquad (7b)$$

Equations 6 and 7 are substituted into eq 3 with the result

$$\frac{\partial(K\,\partial\psi/\partial x)}{\partial x} - K^*\frac{\partial\psi}{\partial x} = \theta^*\frac{\partial\psi}{\partial t} + Q_I \qquad (8)$$

where the primary state variable is ψ. The parameters K, K^*, and θ^* are functions of ψ, and hence eq 8 is nonlinear. Parameter Q_I can be specified a priori or be computed from suitable empirical relationships to be discussed subsequently. (Equation 8 is strictly applicable to moisture flux in unsaturated zones or partially frozen soil and does not apply to a saturated zone; to model a saturated zone or water table in the one-dimensional sense requires an interior interface condition specifying the position of the water table.) Before developing the necessary coupled heat conduction equation, appropriate auxiliary conditions for eq 8 will be presented.

Two types of boundary conditions are considered: *specified boundary conditions and moisture flux boundary conditions*. For the upper boundary,

$$\psi = \psi_U \qquad x = 0 \qquad t > 0$$

$$\frac{\partial\psi}{\partial x} = F_U \qquad x = 0 \qquad t > 0 \qquad (9)$$

where ψ_U is a specified pressure that may be a function of time and F_U is a known function of time (e.g. for a zero flux condition, $F_U = 1$). The lower boundary has similar boundary conditions; i.e.

$$\psi = \psi_L \qquad x = L \qquad t > 0$$

$$\frac{\partial\psi}{\partial x} = F_L \qquad x = L \qquad t > 0. \qquad (10)$$

The remaining auxiliary conditions are initial conditions of the form

$$\psi = \psi_0 \qquad 0 \leq x \leq L \qquad t = 0 \qquad (11)$$

where $\psi_0 = \psi_0(x)$ and is known a priori.

Heat Transport

A rigorous derivation of the heat transport equation can be found in Bird et al. (1960). For purposes of this report a simpler, but correct, derivation will be presented. Most sources (e.g. Meyers 1971) begin by making the deterministic-continuum assumption, which leads to a partial differential equation with temperature as the state variable and with various parameters of state such as heat capacity.

In the model presented here, the first concept employed is that energy is conserved. Thus, by considering the various rate processes involved in a particular process and by maintaining an energy balance on a one-dimensional control volume, the appropriate heat equation is obtained. The various rate processes that might be considered are: conduction, convection, radiation, heat storage, and heat generation (e.g. latent heat effects). In a freezing or thawing soil all of the processes are important. Moreover, the soil water, almost always present, is a dilute solution containing dissolved minerals which affect the soil system's thermal properties. The thermodynamics of soil-moisture systems is treated by Edelfson and Anderson (1943) among others.

The one-dimensional heat transport model is based upon the following assumptions:

1. The presence of dissolved salts does not affect soil thermal properties.
2. Freezing or thawing is an isothermal process and latent heat generation can be accounted for by a "bookkeeping" process.
3. Radiation heat transfer only occurs at the soil/air interface and can be accounted for in the soil surface boundary conditions.
4. Convected heat is primarily in the fluid form and vapor convected heat is negligible.

The energy balance equation is

$$\dot{E}_c + \dot{E}_v = \dot{E}_t \tag{12}$$

where $\dot{E}_c$ is the rate of heat conduction into the elemental volume, $\dot{E}_v$ is the net rate of heat convection into the elemental volume, and $\dot{E}_t$ is the total rate of heat energy stored in the elemental volume. The individual processes in eq 12 are expanded to determine the net heat conduction and convection from the x direction:

$$\frac{q|_{x+\Delta x} - q|_x}{\Delta x}\Delta x - \frac{{}^{\circ}C_w\, v\,(T-T_0)\big|_{x+\Delta x} - C_w\, v\,(T-T_0)\big|_x}{\Delta x}\Delta x = \dot{E}_c + \dot{E}_v \tag{13}$$

where q = heat flux,
Δx = the length of the elemental volume element,
T_0 = a reference temperature,
C_w = the volumetric heat capacity of fluid
v = the fluid flux in the x direction.

The variable q may be replaced by Fourier's law:

$$q_x = -K_T \frac{\partial T}{\partial x} \tag{14a}$$

where K_T is the thermal conductivity of the entire mass of material. Differential equation 14a is then related to the total rate that heat is accumulated in the elemental volume, i.e.

$$\dot{E}_t = C_a \frac{\partial T}{\partial t} \tag{14b}$$

where C_a is the bulk volumetric heat capacity. Combining eqs 13, 14a and 14b, dividing through by Δx, and taking the limit as $x \to 0$, results in

$$\frac{\partial}{\partial x}\left(K_T \frac{\partial T}{\partial x}\right) - \frac{\partial}{\partial x}(C_w\, v\, T) = C_a \frac{\partial T}{\partial t}. \tag{15}$$

The middle term in eq 15, the so-called convection term, may be expanded by the chain rule and the resulting $\partial v/\partial x$ term canceled, because of continuity, to yield

$$\frac{\partial}{\partial x}\left(K_T \frac{\partial T}{\partial x}\right) - C_w\, v \frac{\partial T}{\partial x} = C_a \frac{\partial T}{\partial t}. \tag{16}$$

The model was originally developed using DeVries (1966) method to compute thermal conductivity values (Guymon 1976). Currently the program computes thermal conductivities using Kersten's (1949) equations for soils. Alternatively, the thermal conductivity for each layer can be specified in the initial conditions. Kersten (1949) divided soils and pavement materials into three classes: "fined-grained" (soils consisting primarily of silts and clays), "coarse-grained" (soils consisting primarily of sands and gravels) and "other" (including flexible and rigid pavement materials, insulating layers and soils with high organic contents). Thermal conductivity values for the "other" soil materials must be provided as input to the program, and the initial value input for the material is used throughout the entire time period of the solution. Kersten's equations, presented below, are used for the coarse- and fine-grained soils. In the computer program, thermal conductivity values for a partially frozen element are determined from the equations for frozen soils.

For *unfrozen* fine-grained soils,

$$K_T = [0.9 \log w - 0.1]\ 10^{0.01\gamma_d} \quad (17)$$

and for *frozen* fine-grained soils,

$$K_T = 0.01(10)^{0.22\gamma_d} + 0.085(10)^{0.008\gamma_d}\ (w). \quad (18)$$

For *unfrozen* coarse-grained soils,

$$K_T = [0.7 \log w + 0.4]\ 10^{0.01\gamma_d} \quad (19)$$

and for *frozen* coarse-grained soils,

$$K_T = 0.076(10)^{0.013\gamma_d} + 0.032(10)^{0.0146\gamma_d}\ (w). \quad (20)$$

These are empirical equations where γ_d is dry weight (lb/ft^3), w is the total moisture content (water plus ice % dry weight), K_T is thermal conductivity (Btu/ft h °F).

Since the remainder of the computer program uses data in the cgs system of units, dry unit weights are converted from g/cm^3 to lb/ft^3 to compute the thermal conductivity, and then the thermal conductivity is converted from Btu-in./ft^2 h °F to cal/cm h °C. Moisture contents are converted from volumetric percentages to percentages on a dry weight basis for the thermal conductivity calculations.

A method similar to that suggested by Kersten (1949) is used to compute the volumetric heat capacity of the soil-water-ice mixture. The equation used to calculate the specific heat of the mixture is

$$c_m = (100\, c_s + w\, c_w + w_i\, c_i)/(100 + w_t) \quad (21)$$

where c_m = specific heat of the mixture
c_s = specific heat of the soil
w = liquid moisture content, % dry weight
c_w = specific heat of water
w_i = ice content, % dry weight
c_i = specific heat of ice.

The volumetric heat capacity C_a is determined simply by multiplying the specific heat of the mixture by the bulk density of the soil-water-ice mixture.

The volumetric latent heat of fusion is computed from

$$L = h_f\, \gamma_d\, (w_t - w_u) \quad (22)$$

where L = volumetric latent heat of fusion
h_f = heat of fusion of water
γ_d = dry unit weight of soil
w_t = total water content (water plus ice), % dry weight
w_u = unfrozen water content, % dry weight.

DeVries (1966 and 1952) and others have proposed additional empirical relationships for some of these auxiliary equations. Because they are not essential to the governing equation of state, the numerical solution procedure developed here can easily be modified to accommodate different auxiliary equations; i.e. they can be "plugged into" the main system model much like appliances are plugged into an electrical circuit.

Because water storage and movement and thermal states are assumed to be coupled throughout the entire soil column, it is necessary to specify boundary conditions at the same boundaries as used for the moisture transport equation. This situation presents a problem at both ends of the column, since at the ground surface (i.e. $x = 0$) heat is added or lost by radiation and convection as well as by conduction. Moreover, the temperature or its gradient at $x = L$ may not be known at the same point that the boundary condition for moisture flux is known. Both difficulties could be theoretically overcome by establishing two different solution domains; however, such a procedure would make programing complex. Accordingly, these difficulties will be ignored, and boundary conditions of the following type will be used:

$$T = T_U \qquad x = 0 \qquad t > 0$$

$$\frac{\partial T}{\partial x} = H_U \qquad x = 0 \qquad t > 0 \quad (23)$$

and

$$T = T_L \qquad x = L \qquad t > 0$$

$$\frac{\partial T}{\partial x} = H_L \qquad x = L \qquad t > 0 \quad (24)$$

where U and L indicate upper and lower boundary conditions, respectively. The upper and lower thermal boundary conditions must be located at the same positions as the corresponding moisture flux boundary conditions. The upper or lower specified temperature may be a function of time, and H indicates a specified heat flux function that may be time-dependent. Additionally, eq 12 and certain of its auxiliary equations require initial conditions of the following type:

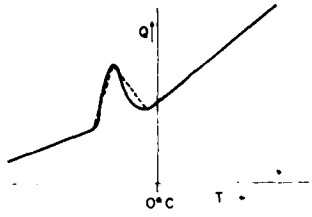

a. Apparent heat capacity.

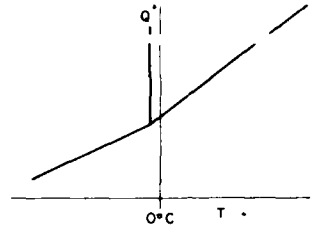

b. Isothermal freezing.

Figure 3. Schematic representation of two phase change algorithms.

$$T = T_0 \qquad 0 < x < L \qquad t = 0 \qquad (25)$$

and $$\theta = (\theta)_0 \qquad 0 < x < L \qquad t = 0. \qquad (26)$$

Phase Change

Phase change is the major heat transport phenomenon associated with freezing and thawing of soils. One method of including the effect of phase change is to use an "apparent heat capacity" over a subfreezing temperature range (Anderson et al. 1973, Johansen 1977). This concept is shown schematically in Figure 3a. Since different soils have various curves in the freezing zone, Johansen (1977) suggested using two straight lines as shown in the figure to approximate freezing within this temperature range. Since moisture flux and formation of ice lenses could cause the apparent heat capacity and computed temperatures in the freezing zone to vary in an indeterminate fashion, a simpler procedure assuming isothermal freezing (Fig. 3b) was used in this model. Hromadka and Guymon (in prep.) state that the apparent heat capacity concept does not converge near $T = 0°C$, and that time steps required for sufficiently accurate solutions are very small.

We assume that all of the water available for freezing does so at a temperature somewhat below the freezing point of pure bulk water. The freezing point depression is an input parameter for the computer program as is the amount of unfrozen water. The unfrozen water content depends primarily on the grain-size distribution of the soil particles and can be determined by any of several methods (McGaw and Tice 1976, Anderson and Tice 1972, Keune and Hoekstra 1967).

A procedure similar to the concept of "excess degrees," (Dusinberre 1961) was used to locate the freezing front. This method requires a bookkeeping process to ascertain the location of the freezing front. It is also similar to the procedure used by Bafus and Guymon (1976).

The amount of heat which must be removed to freeze an element is determined from the product of volumetric latent heat of fusion L of the soil water within an element and the volume of the element V. The amount of heat required to change the average temperature of an element by one degree is the product of the volumetric heat capacity C_a and the volume of the element. If the first product, $L \times V$, is divided by the latter, $C_a \times V$, the number of "excess degrees" E required to freeze the element is obtained.

This approach is illustrated by considering a common point (node) A in a discretized one-dimensional domain. Phase change is not permitted to occur at node A until the requisite amount of latent heat has been exhausted or added. The prevailing quantity of latent heat for node A is determined as described above. The volume of the soil, water and ice mixture associated with each point consists of a finite element of the mixture atop node A. After each time increment where a solution is generated, the temperature of point A is scanned to determine whether or not it has dropped below a prescribed temperature where phase transformation is assumed to occur—the freezing point depression T_d. If the node has not been entirely frozen and the computed temperature has dropped below T_d, then the quantity of excess degrees evolved during the previously computed time step becomes

$$E_t = T_d - \text{computed temperature} \qquad (27)$$

where E_t represents the excess degrees removed from node A during the previous time step.

The quantity E_t is subtracted from the latent heat (excess degree) accumulator for point A, and if more latent heat must still be exhausted, the computed temperature at the node is brought back to T_d prior to obtaining a new solution. This is analogous to simulating phase change as an isothermal process.

If the required amount, or more than the required amount of latent heat has been extracted, node A and the volume of soil water assigned to it are considered to be frozen. The thermal properties of the volume

common to node A are then updated based on the volumetric proportions of soil water and soil ice present in the respective elements. If an excess amount of latent heat is removed, the residual is used to calculate the value of the temperature which is now below T_d.

Since the moisture content and thus the volumetric latent heat of fusion and volumetric heat capacity may change during each time step, values of these parameters are recomputed after each time increment. Other parameters are updated at a frequency specified in the initial input data. Additional discussion of the phase change algorithm is contained in the section *Evaluation of the Mathematical Model*.

The thawing process is handled in a similar manner. Provisions are made to determine which points are frozen or thawed so as to avoid refreezing frozen areas. Boundary conditions remain unaffected by the checking routines that scan point temperatures. After phase transformation at a point occurs, the latent heat accumulator assigned to that point is recomputed. Recomputation permits the simulation of long-term cyclic freezing and thawing.

Coupling Effects

The equation for fluid (water) flux in a freezing or thawing soil adopted in this report is eq 8 with appropriate boundary conditions as discussed above. The equation of heat flux in a freezing or thawing soil adopted in this report is eq 16 with its associated boundary conditions. These two equations are coupled together, especially in a freezing and thawing soil, because of the parameters that arise in the equations.

Considering eq 8 first, each term of this equation is coupled to eq 16 by virtue of the parameters K, K^*, θ^*, and Q_l, which are dependent upon temperature while a soil is freezing or thawing. Similarly, each term of eq 16 is coupled to eq 8 because its parameters k_T, ν, and C_a depend upon water content.

In a highly dynamic system, this coupling would present a formidable problem. However, the natural soil systems considered here are highly damped. Even soil columns rapidly frozen in the laboratory may be considered reasonably damped. This is fortuitous since it will allow the momentary decoupling of the governing equations of state. Consequently, one equation can be solved while holding its parameters constant for a time period and then the other equation can be solved while holding its parameters constant. Parameters can be updated at any arbitrary frequency in the computation procedure to provide the desired level of precision.

Frost Heave Algorithm

The frost heave algorithm consists of two components: the first is used to compute the actual frost heave during the previous time increment and the second component to define the pore water pressure (tension) at the freezing front.

The first component is comparatively simple. The porosity of each soil layer, and therefore for each element in the mathematical simulation, is provided in the input data. At each time increment, the heat available for freezing additional water is computed. If the volume of water available for freezing is greater than 90% of the porosity, frost heave occurs [Dirksen and Miller (1966) used a value of 85% in their study]. The magnitude of this incremental amount of frost heaving is determined by multiplying the amount of newly frozen water in excess of 90% of the porosity by 1.09. Thus we assume that all of the volume change is in the vertical direction and that the width and depth of the frozen increment are both 1 cm in length. We also assume that all water which enters the freezing element travels to the freezing front; i.e. the moisture content of the unfrozen portions of the element remains unchanged.

The second component of the frost heave algorithm is based on a capillary model discussed by several authors, e.g. Everett (1961), Penner (1957), Gold (1957), Williams (1967) and McRoberts and Nixon (1975). The capillary model is based on the premise that the ice/water interfaces in soil pores are curved. A pressure difference occurs at the boundary due to the energy of the interface. The pressure difference is

$$P_i - P_w = \frac{2\,\sigma_{iw}}{r} \tag{28}$$

where P_i = stress on the ice
P_w = pore water pressure
σ_{iw} = ice/water surface tension (30.5 dynes/cm)
r = equivalent pore radius of the soil.

The pressure on the ice may be assumed equal to the overburden stress and surcharge loading (Williams 1967). Thus

$$P_i = S + \sum_{j=1}^{n} \gamma_j\, d_j \tag{29}$$

where S = surcharge stress
γ_j = bulk density of soil layer j
d_j = thickness of soil layer j.

The bulk density of a soil layer changes with time as water flows into or out of the layer. It also changes as ice accumulates in the layer. In the mathematical model, each element is considered as an individual layer.

The equivalent critical pore radius of the soil is estimated from the soil moisture characteristic curve (desorption portion). The empirical criteria of Hoekstra et al. (1965) are applied to correlate maximum heaving pressure developed by a soil with its moisture characteristic curve using the following reasoning:

> The maximum pressure will be developed in order for the ice interface to proliferate through the smallest pores. However, it is clear that this cannot be the only criterion; the number of small pores present is another. If there were only a few pores of a small size present, the freezing front could bypass them. The amount of water held in pores of a particular size range is given by the slope...[of the moisture characteristic curves].

They suggested that the tension P_c at the point where the slope of the tension vs percent saturation curve decreased rapidly was an indicator of the maximum heaving pressure of a soil. The same point was used to define the effective critical pore radius in this study. The following equation was used to determine the radius:

$$r_c = -\frac{2\,\sigma_{aw}}{P_c} \qquad (30)$$

where r_c = was defined above
σ_{aw} = air/water surface tension (72.75 dynes/cm at 20°C)
P_c = critical soil water pressure from moisture characteristic curve.

Penner (1959) stated that the maximum overburden pressure to stop heaving appeared to be about twice as great as the maximum soil water tension required to stop heaving. His statement was based on results from laboratory tests that he had conducted and from data reported by Beskow (1935). Equation 28 does not suggest how, or if, the pressure should be partitioned. Based on Penner's comment, however, we arbitrarily doubled the effect of the pore water pressure in the equation.

All the referenced observations were included in an equation for computing the pore water tension (suction) at the freezing front:

$$2P_w = P_i - \frac{2\,\sigma_{iw}}{r_c} \qquad (31)$$

or by combining eq 29, 30, and 31

$$P_w = 1/2\,[(S + \sum_{j=1}^{n} \gamma_j\, d_j) + \sigma_{iw}\, P_c/\sigma_{aw}]. \qquad (32)$$

The effects of overburden and surcharge, if any, are taken into consideration by the first term within the brackets. This equation is used to compute the soil water suction at the freezing front. Generally, this pressure "drives" the water movement in the system and it can be considered a moving boundary condition. Once an element is completely frozen, it is considered that water does not flow within it; i.e. no moisture flows in the frozen zone.

Using the equation presented above, we may compute soil water tension after each time step. As water flows into the freezing element from below, the degree of saturation of the soil voids increases. When saturation exceeds 90%, heaving commences within the element. The amount of heaving is equivalent to 9% of the volume of water up to 90% saturation and 109% of the water exceeding a degree of saturation of 90%.

It is evident from the above discussion that no heaving occurs behind the freezing front in this model. In laboratory studies, several authors have observed increased water contents in the frozen soil (Dirksen 1964, Dirksen and Miller 1966, Hoekstra 1966, Jame and Norum 1976). Loch and Kay (1978) reported that laboratory data indicate ice lenses form slightly behind the freezing isotherm in a silty soil. Taylor and Luthin (1978) permit moisture flux in frozen soil, but the laboratory test results that they simulated did not exhibit frost heave.

Subsurface frost heave gages were recently installed in a field test section at CRREL. The soil was a silty sand and data from the heave gages indicate that heaving continued at temperatures substantially below freezing. Kinosita (1975) also installed subsurface frost heave gages in test sections, and his data indicate a significant amount of frost heave within the frozen zone. At this time it is not possible to formulate equations for estimating the amount of heave within the frozen zone. Miller* has recently received funds for studying and formulating his hypothesis of "secondary heaving" and significant effort will be expended by him in the next few months. When a formulation for heaving within a frozen soil is accomplished it may be incorporated into the existing model.

DEVELOPMENT OF COMPUTER MODEL

The purpose of this section of the report is to develop general solutions to the fluid flux and storage equation and the heat transport equation.

*R.D. Miller, Cornell University, Personal Communication 1978.

So-called analytical closed form solutions may be found for partial differential equations provided the domain of solution, the boundary and initial conditions, and the parameters are such that a particular solution can be found. As a matter of interest no such solution has ever been found for the fluid flux and storage equation developed in the preceding section. Only a limited number of analytical solutions have been found for the heat transport equation. Because the domain of interest is of arbitrary finite length, the boundary conditions variable in time and space, and the parameters nonlinear (i.e. depending on the moisture and temperature state), the only possible solution is a so-called general solution. General solutions imply both spatial and temporal discretization and other approximations associated with parameters. Because the computational effort is usually large for most practical problems of interest, the general solution must usually be a numerical solution using a computer. Although analog computers can be used, most solutions are found by digital computers.

Such an approach was used in this study. The model was prepared for a modern high speed computer using FORTRAN IV as a programing language. The model has been run on a PDP-10 at the University of California (Irvine), on an IBM 370/155 in southern California, and on the Honeywell system at Dartmouth College. Before the model could be programed, however, the partial differential equations had to be reduced to a numerical analog suitable for computer programing.

The most efficient numerical analogs for solving partial differential equations involve deterministic approaches as opposed to stochastic methods. The two basic deterministic approaches are the finite difference method and the finite element method.

Finite Difference vs Finite Element Method

To simplify the comparison of the two methods, the partial differential equations were simplified to normalized symmetrical parabolic equations of the type

$$\frac{\partial^2 u}{\partial x^2} = \frac{\partial u}{\partial t} \tag{33}$$

so that analytical solutions could be derived in order to compare with the numerical analogs. For the boundary and initial conditions

$$u(0, t) = a; u(1, t) = b; t > 0$$

$$u(x, 0) = f(x), 0 < x < 1$$

an analytical solution is easily obtained (Meyers 1971). Such a solution is used here for comparison purposes.

First, we will consider the various finite difference schemes investigated. The finite difference method approximates the partial derivatives found in the boundary and initial value problem by *direct substitution* of a finite difference between solution end points for the continuous partial differential operator. There are two basic approaches for doing this: the explicit difference method and the implicit difference method. The procedure will be illustrated by considering the explicit technique.

Let u in eq 33 be a single valued, finite, and continuous function of x such that u can be expanded in Taylor's series

$$u(x+h) = u(x)+hu'(x)+\frac{h^2}{2!}u''(x)+...$$

$$u(x-h) = u(x)-hu'(x)+\frac{h^2}{2!}u''(x)-...$$

where $h = \Delta x$. By assuming that fourth and higher powers of h are negligible, the above can be combined to yield

$$u(x+h)+u(x-h) = 2u(x)+h^2u''(x),$$

or rearranging this result

$$u''(x) = \left.\frac{d^2u}{dx^2}\right|_x = \frac{1}{h^2}\left[u(x+h)-2u(x)+u(x-h)\right]. \tag{34}$$

Since u is also a function of time t [i.e. $u = u(x, t)$] a suitable finite difference approximation for $\partial u/\partial t$ must be found, e.g.

$$\frac{du}{dt} = \frac{u(t+k)-u(t)}{k} \tag{35}$$

where $k = \Delta t$.

Now if the x space is descretized into equal increments h and the t space is descretized into equal increments k, we can adopt a standard subscript notation which specifies the solution u at a particular point i in space or a particular point j in time; i.e. $u = u_{i,j}$. Equations 34 and 35 are combined as a finite difference analog for eq 33 and the i, j subscript notation is adopted to yield

$$u_{i,j+1} = \frac{k}{h^2}(u_{i+1,j}-2u_{i,j}+u_{i-1,j})-u_{i,j}. \tag{36}$$

That is, u at point i in space and at time $j+1$ is explicitly determined by values of u (at spatial points

$i+1$, i, and $i-1$) that were computed in the previous time step j. For eq 36 to converge (Meyers 1971)

$$\frac{k}{h^2} < \frac{1}{2}$$

Other finite difference schemes investigated include the implicit method

$$\frac{1}{k}(u_{i,j+1}-u_{i,j}) = \frac{1}{2}\left[\frac{1}{h^2}(u_{i+1,j+1} - 2u_{i,j+1}+u_{i-1,j+1}) + \frac{1}{h^2}(u_{i+1,j}-2u_{i,j}+u_{i-1,j})\right] \quad (37)$$

where $k/h^2 < \infty$.

These two basic methods were solved using various techniques consisting of initial boundary value problems with derivative boundary conditions: Gauss elimination, Gauss-Seidel iteration, and solution by successive over-relaxation. [These solution techniques were also compared to a finite element analog for the same equation (eq 33) and will be discussed in detail in the next section.]

The results of this evaluation are qualified since program efficiency is dependent upon coding techniques. For example, one programer may be able to develop a finite difference program that is much more efficient than another; i.e. efficiency is defined as computer execution time vs solution precision.

In general the results indicated that the finite difference techniques studied required a substantial number of iterations to reach a stable accurate solution. Time steps had to be correspondingly smaller than the finite element methods which did not exhibit stability problems. The difference in computer execution time was inconclusive for the one-dimensional problem studied. Because of the need for iteration in the implicit schemes and the requirement for smaller time step sizes, it is probable that two- and three-dimensional solutions by the finite element method would be superior to finite difference methods. The main advantage of the finite element method is considered to be the ability to deal with complex and arbitrary boundary conditions. Thus, for the one-dimensional case it is considered a toss-up as to which method is better. However, because the model is planned to be extended to the two-dimensional case, the finite element method is advantageous for the reasons mentioned above.

Finite Element Formulation

The heat equation and moisture flux equation have the general form

$$k_1 \frac{\partial^2 u}{\partial x^2} - k_2 \frac{\partial u}{\partial x} = k_3 \frac{\partial u}{\partial t} - k_4 \quad (38)$$

where the parameters k_i are the heat equation parameters or the moisture pressure state parameters. The state variable u is either the temperature or the pore water pressure. The reason for writing the coupled heat and moisture state equations in the above form is to clearly indicate that the two equations are identical in form and to facilitate the derivation of their finite-element analog.

We wish to apply the Galkerin method which is a special case of the general method of weighted residuals. To explain the concept, consider a general operator A which is positive definite. Suppose A operates on the continuous function u as follows:

$$Au = f. \quad (39)$$

Now we seek an estimate of u, which we will call $\hat{u}$, such that $\hat{u}$ approximately solves the above; i.e.

$$A\hat{u} \simeq f$$

where $\hat{u}$ can be represented as the product of an appropriate shape function $\langle N \rangle$ and the value of the state variable at required model points $\{u\}$; i.e. $\hat{u} = \langle N \rangle \{u\}$. We know that the equation will not be exactly solved by $\hat{u}$ so that we have a "residual" error; i.e.

$$A\hat{u} - f = r$$

where r is some small error. Since this small unknown error varies over the space in which A defined, let us think of it as a weighted average error that we minimize. We can minimize r as follows:

$$\int \langle N \rangle^T (A\hat{u} - f)\, dx = 0 \quad (40)$$

and find $\hat{u}$. The value of $\hat{u}$ obtained will be our best estimate of u such that r is minimum.

Using eq 38, eq 40 becomes

$$\int_0^L \langle N \rangle^T \left[k_1 \frac{\partial^2 u}{\partial x^2} - k_2 \frac{\partial u}{\partial x} - k_3 \frac{\partial u}{\partial t} + k_4\right] dx = 0 \quad (41)$$

where L is the total length of the domain of solution and $\langle N\rangle^T$ is the transpose of the weighting functions (shape functions) to be described later. In eq 41 and in subsequent equations, u is the $\hat{u}$ approximation and is used to avoid the $\hat{}$ notation. Before proceeding further, it is convenient to modify eq 41 so that if the state variable u is approximated by a linear shape function, $u = \langle N\rangle \{u\}$, the first term of the integrand of eq 41 will not vanish. A suitable adjustment is made by integrating the first term of eq 41 by parts, i.e.

$$\int_0^L \langle N\rangle^T k_1 \frac{\partial^2 u}{\partial x^2}\,dx = k_1 \int_0^L \langle N\rangle^T \frac{\partial}{\partial x}\left(\frac{\partial u}{\partial x}\right)dx$$

$$= k_1 \left(\langle N\rangle^T \frac{\partial u}{\partial x}\bigg|_0^L - \int_0^L \frac{\partial u}{\partial x}\frac{\partial \langle N\rangle^T}{\partial x}dx\right). \tag{42}$$

The first term in the result is associated with the boundary conditions where $\partial u/\partial x = 0$ on the boundary if u is specified. If u is not specified, $\partial u/\partial x \to 0$; hence it is called a natural boundary condition since it is automatically satisfied. Ignoring the boundary conditions for the time being and substituting the second term of eq 42 into 41 and multiplying through by -1, we have

$$\sum_{m=1}^{M} \int_0^{\ell} k_1 \frac{\partial \langle N\rangle^T}{\partial x}\frac{\partial u}{\partial x} + k_2 \langle N\rangle^T \frac{\partial u}{\partial x}$$

$$+k_3 \langle N\rangle^T \frac{\partial u}{\partial t} - k_4 \langle N\rangle^T \quad dx = 0 \tag{43}$$

where the solution domain, $0 < x < L$, has been divided into M finite elements of length ℓ. Substituting the shape function $u = \langle N\rangle \{u\}$ into eq 43 yields

$$\sum_{m=1}^{M} \int_0^{\ell} \left(k_1 \frac{\partial \langle N\rangle^T}{\partial x}\frac{\partial \langle N\rangle}{\partial x}\{u\}\right.$$

$$+k_2 \langle N\rangle^T \frac{\partial \langle N\rangle}{\partial x}\{u\}$$

$$\left.+k_3 \langle N\rangle^T \langle N\rangle \{\dot{u}\} - k_4 \langle N\rangle^T\right) dx = 0 \tag{44}$$

where the dot in $\{\dot{u}\}$ indicates differentiation with respect to time t.

In the finite-element method, a solution of the problem is obtained by specifying an approximation of the state variable in each finite element of the domain such that 1) the state variable is continuous throughout the entire domain, 2) the first derivative with respect to space exists in each element (but not necessarily on the element interfaces), and 3) the boundary conditions are satisfied. These last three conditions are called "admissibility requirements." First, consider the solution domain divided into M finite elements as follows:

Elements

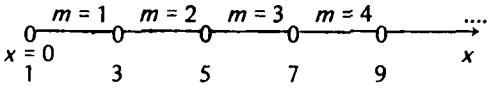

Nodes

Consider the *mth* element as follows:

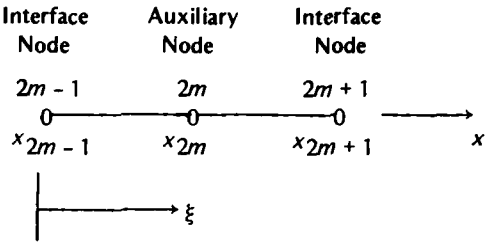

where x is the global coordinate and ξ is the local coordinate. An auxiliary node is included and will be explained shortly. The relationship between coordinates is given by

$$\xi = x - x_{2m-1}.$$

The length of the *mth* element is

$$\ell = x_{2m+1} - x_{2m-1}$$

and node $2m$ is at the midpoint of the element. We wish to approximate the state variable u by a second order polynomial (quadratic shape function) as follows:

$$u = a + b\xi + c\xi^2 = [1\ \xi\ \xi^2]\begin{vmatrix} a \\ b \\ c \end{vmatrix}. \tag{45}$$

The unknown coefficients (a, b, and c) can be determined if there are three independent, simultaneous equations to solve; hence, the purpose of the midpoint node:

$$u_{2m-1} = [1\ 0\ 0]\begin{vmatrix} a \\ b \\ c \end{vmatrix}$$

$$u_{2m} = [1 \; \ell/2 \; \ell^2/4] \begin{vmatrix} a \\ b \\ c \end{vmatrix}$$

$$u_{2m+1} = [1 \; \ell \; \ell^2] \begin{vmatrix} a \\ b \\ c \end{vmatrix}$$

which can be formed into a 3x3 matrix

$$\begin{vmatrix} u_{2m-1} \\ u_{2m} \\ u_{2m+1} \end{vmatrix} = \begin{vmatrix} 1 & 0 & 0 \\ 1 & \ell/2 & \ell^2/4 \\ 1 & \ell & \ell^2 \end{vmatrix} \begin{vmatrix} a \\ b \\ c \end{vmatrix}.$$

Taking the inverse of the 3x3,

$$\begin{vmatrix} a \\ b \\ c \end{vmatrix} = \begin{vmatrix} 1 & 0 & 0 \\ -3/\ell & 4/\ell & -1/\ell \\ 2/\ell^2 & -4/\ell^2 & 2/\ell^2 \end{vmatrix} \begin{vmatrix} u_{2m-1} \\ u_{2m} \\ u_{2m+1} \end{vmatrix}$$

and substituting this into eq 47 gives

$$u = [1 \; \xi \; \xi^2] \begin{vmatrix} 1 & 0 & 0 \\ -3/\ell & 4/\ell & -1/\ell \\ 2/\ell^2 & -4/\ell^2 & 2/\ell^2 \end{vmatrix} \begin{vmatrix} u_{2m-1} \\ u_{2m} \\ u_{2m+1} \end{vmatrix} \quad (46)$$

By matrix multiplication the above can be written as

$$u = \frac{1}{\ell^2} [\ell^2 - 3\ell\xi + 2\xi^2, \; 4\ell\xi - 4\xi^2, \; -\ell\xi + 2\xi^2] \begin{vmatrix} u_{2m-1} \\ u_{2m} \\ u_{2m+1} \end{vmatrix} \quad (47)$$

which can also be written as

$$u = \langle N \rangle \{u\} \quad (48)$$

where u is the state variable in terms of the nodal displacements $\{u\}$, $\langle N \rangle$ is a 1x3 matrix which is a function of ℓ only, and $\{u\}$ is a column matrix of the nodal state variable values.

Returning to eq 44, it is integrated term by term to obtain the desired result which consists of a matrix equation of the form

$$[s] \{u\} + [p] \dot{u} = \{f\} \quad (49)$$

which is derived in detail in Appendix C. This element system equation is appropriately assembled with all other system equations, as is indicated in the appendix, to form the system equation

$$[S] \{u\} + [P] \{\dot{u}\} = \{F\} \quad (50)$$

where $[S]$ is a square banded nonsymmetrical matrix, $\{u\}$ is a column matrix of nodal unknowns, $\{\dot{u}\}$ is the ordinary time derivative, and $\{F\}$ is a column matrix. The $[S]$ matrix is determined by the geometry of the discretization in space and the conductivity parameter. $[P]$ is determined by spatial discretization and the capacitance parameter. $\{F\}$ is determined by the ice sink term and the boundary conditions. As is indicated in Appendix C, special computer storage of eq 50 is possible to minimize storage requirements. Equation 50 represents a system of ordinary equations which must be solved with respect to time.

Time Domain Solution

Once system matrices have been constructed in the finite-element formulation of a parabolic partial differential equation, the problem becomes one of solving the linear first order differential equations given by eq 50. The Crank-Nicholson method of solution is utilized here and consists of an arithmetic mean of the derivative of the state variable at the beginning and end of each time step to move the solution ahead in time. Thus

$$\{u\}^{v+1} = \{u\}^{v} + \frac{\Delta t}{2} \left(\{\dot{u}\}^{v} + \{\dot{u}\}^{v+1} \right) \quad (51)$$

where v is the time step.

Premultiplying by the $[P]$ matrix, this becomes

$$[P]\ \{u\}^{v+1} = [P]\ \{u\}^{v} + \frac{\Delta t}{2}$$

$$\left([P]\ \{\dot{u}\}^{v} + [P]\ \{\dot{u}\}^{v+1}\right). \qquad (52)$$

But

$$[P]\ \{\dot{u}\} = \{F\} - [S]\ \{u\}. \qquad (53)$$

Therefore,

$$[P]\ \{u\}^{v+1} = [P]\ \{u\}^{v} + \frac{\Delta t}{2}$$

$$\left(\{F\} - [S]\ \{u\}^{v} + \{F\} - [S]\ \{u\}^{v+1}\right)$$

$$[S] + \frac{2}{\Delta t}[P]\ \{u\}^{v+1}$$

$$= \left(\frac{2}{\Delta t}[P] - [S]\right)\ \{u\}^{v} + 2\ \{F\}.$$

Since $\{u\}^{v}$ would be the initial conditions of a problem or previously computed values of the state variable, the above equation can be reduced to

$$[W]\ \{u\}^{v+1} = [Z]\ \{u\}^{v} + 2\ \{F\}$$

$$[W]\ \{u\}^{v+1} = \{G\} \qquad (54)$$

where $\{u\}^{v+1}$ is computed by Gaussian elimination.

EVALUATION OF THE MATHEMATICAL MODEL

Evaluation of the model is being accomplished in two phases: 1) study of the accuracy of the finite element approach as applied to problems where the governing equations of state are known and exact solutions are available, and 2) study of the validity of assumptions necessary to extend the model to problems where the equations of state and their solutions are not known. Evaluation of the model has proceeded step by step.

In our work, we have verified by demonstration rather than by theoretical analysis. Initial and boundary conditions for which analytical solutions are available have been used to evaluate and verify portions of the model. Comparisons with laboratory experiments have been made to evaluate and refine other portions of the model. Initially heat and moisture flux portions of the model were "decoupled" to evaluate each portion individually. Decoupling was accomplished by choosing heat or moisture flux parameters which effectively caused no moisture flux when evaluating the heat flow portions and vice-versa. The following sections initially discuss the decoupled evaluations and lastly the coupled model using both laboratory and field test results for comparison.

Heat Flux

The heat flux portion of the model was compared with analytical solutions for two different problems in which phase change does not occur. In both cases the convective heat transfer contributions have been set to zero, and the moisture flow part of the coupled equations has, in effect, been neglected. In these comparisons, the volumetric heat capacity was 0.582 cal/cm^3 °C and the thermal conductivity was 16.05 cal/cm h °C, typical values for a silty soil. First the model was compared to an analytical solution for the transient temperature distribution in a homogeneous semiinfinite body initially at a uniform temperature with a step change of 20°C applied to the upper surface of the body. Figures 4 and 5 show the maximum deviation of the finite element method (FEM) solution (using linear shape functions) from the analytical solution for several different combinations of element lengths and time increments in elapsed times of 1 and 10 hours. In Figure 4 the time increment is 0.1 h while the element length (uniform over the entire spatial domain) is varied. A progression toward smaller elements initially decreases the maximum error, but after some apparently optimum element length, approximately 2 cm, the trend is reversed and larger errors again occur. It is important to note, however, that these errors occur at nodes just below the forced upper boundary (column 4 in Table 1) and that the error decreases quickly with depth. Table 1 illustrates that the accuracy at an arbitrarily chosen depth of 10 cm steadily improved as the element length decreased, although the maximum error increased between element lengths of 2.0 to 1.0 and 1.0 to 0.5 cm.

As indicated in Figure 5, shrinking the time increment decreased the maximum error, although the rate of improvement became insignificant rather quickly.

Table 2 provides another perspective regarding errors associated with time discretization. The fourth column shows depths at which the maximum errors occurred. This depth increased as the maximum error decreased, indicating that the initial error was propagated downward through the profile in successive time increments. The fifth column contains errors at a depth of 10 cm. The relatively small error corresponding to a time increment of 0.5 hours is deceptive. Since a large negative error exists at a depth of 8.0 cm and a large positive error exists at 12.0 cm (these data are not shown in this report), the error observed at 10.0 cm falls, by coincidence, near the intersection of the FEM and

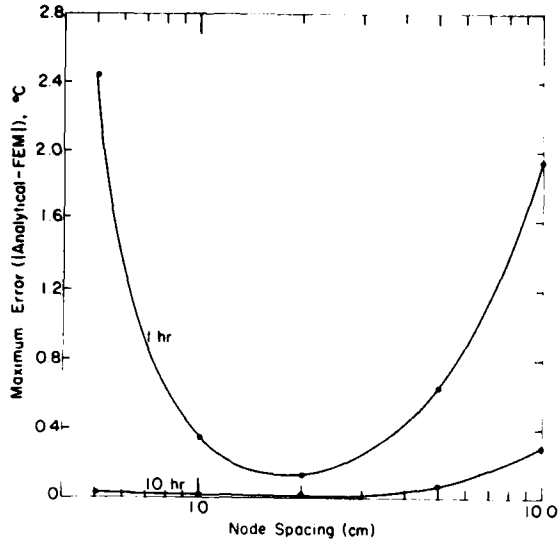

Figure 4. Maximum errors after 1 and 10 hours of simulation for various element lengths and a time increment of 0.1 hr.

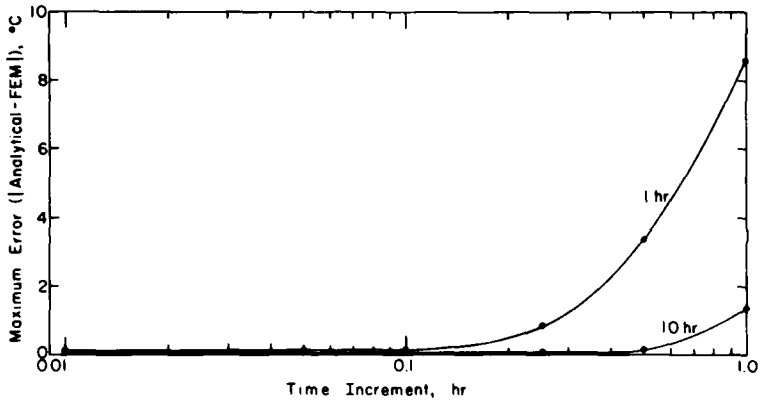

Figure 5. Maximum errors after 1 and 10 hours of simulation for various time increments and element lengths of 2 cm.

Table 1. Errors after one hour for various element lengths and a constant time increment.

Element length (cm)	*Time increment (h)*	*Maximum error* in profile (°C)*	*Depth at which max. error occurs (cm)*	*Error at 10.0-cm depth (°C)*
10.0	0.1	-1.952	10.0	-1.952
5.0	0.1	-0.638	5.0	-0.537
2.0	0.1	-0.126	6.0	-0.084
1.0	0.1	-0.346	2.0	-0.021
0.5	0.1	-2.448	0.5	-0.005

*Error = analytical solution - FEM solution.

Table 2. Errors after one hour for various time increments and a constant element length.

Element length (cm)	Time increment (h)	Maximum error* in profile (°C)	Depth at which max. error occurs (cm)	Error at 10.0 cm (°C)
2.0	1.0	-8.610	2.0	-0.813
2.0	0.5	+3.400	2.0	+0.088
2.0	0.25	-0.807	4.0	-0.131
2.0	0.1	-0.126	6.0	-0.084
2.0	0.05	-0.122	6.0	-0.074
2.0	0.025	-0.120	6.0	-0.084
2.0	0.01	-0.120	6.0	-0.084

*Error = analytical solution - FEM solution

analytical solutions. This simple error analysis provides some insight into the performance of the model. However, a root mean square error analysis on the accuracy of the finite element method with second-order shape functions has been performed for a similar problem and provides a different perspective of computational errors. In the finite element solutions, the overall accuracy improved rapidly as the spatial increment was made smaller, until the root mean square error was essentially zero. A similar trend was observed when the size of the time increment was decreased, although in both cases, the error near the forced boundary condition may have been considerable. Data also indicate that second order shape functions use less computer run time in achieving a given level of accuracy than do linear shape functions.

It is important to note that a surface temperature step change of 20°C is a severe test of the model, and that a step change of this magnitude will rarely be observed in actual road or airfield pavements. Nonetheless, the attainable accuracy is well within engineering requirements. In addition, our studies have shown that, for all combinations of spatial and temporal discretization, a smaller surface temperature step change caused correspondingly smaller errors; in fact, if the magnitude of the step change were decreased by one-half, the new error would be significantly less than one-half the previous error.

The heat flow portion of the finite element model was also compared with the analytical solution to the problem where the surface temperature varied sinusoidally. The temperature of the semi-infinite body was initially uniform at the mean temperature of the sinusoid. Again, phase change was not considered. The sinusoid was approximated in the computer simulation by a series of step changes, occurring at each discrete time interval. The overall error decreased with time for both the linear and second-order shape functions, although the error at the node directly below the surface occasionally increased slightly. The largest errors occurred after the largest step changes; with constant time increments this happened whenever the argument of the sine function was a multiple of π. The overall accuracy of the solution was especially sensitive to the size of the time increment because 1) smaller time increments cause smaller step changes and better representation of the sinusoid, and 2) the Crank-Nicholson method leads to better convergence. Again, second-order shape functions appeared to be more efficient (required less computer run time for a given level of accuracy) than linear shape functions.

The phase change algorithm is an extension of the heat flow problem; again the convective contribution was effectively set to zero for this evaluation. Table 3 contains the differences between solutions obtained from the modified Berggren equation and those obtained using the FEM model (with linear shape functions) for seven representative combinations of time increment size and node spacing. Thermal properties of the soil used in this evaluation are slightly different from those used previously and are shown in Table 3. The ratio of latent heat accumulated to the total heat extraction necessary for complete freezing was used to approximate the position of the freezing front within the element. Data indicate that decreasing the size of the element does not necessarily improve the accuracy of the solution. There are two reasons for this: 1) the algorithm is not adequate if the rate of frost penetration is such that the freezing front advances more than one element in a single time increment, and 2) the first part of the two-step algorithm may yield physically unrealistic temperatures if the time increment is too large relative to the element size. A further complication is that the accuracy of the solution does not necessarily improve if the time increment size is decreased while the element length is held constant. The reasons for this behavior are not entirely clear, but most of the error occurs during

Table 3. Errors in frost depth calculations using linear shape functions.*

Elapsed time (h)	Analytical solution (modified Berggren equation) (cm)	Difference between analytical solution and FEM solution (analytical - FEM). (cm)						
		Node spacing (cm)	0.5	2.0	2.0	1.0	2.0	5.0	10.0
		Time increment (h)	0.02	0.1	0.25	0.5	0.5	0.5	0.5
1	2.28		-0.06	-0.45	+0.14	1.00	0.68	-0.02	-1.57
2	3.23		-0.06	-0.77	-0.01	0.94	0.73	-1.37	-4.46
3	3.96		-0.06	-0.67	-0.13	0.94	0.56	-1.32	-6.04
4	4.57		-0.06	-0.75	-0.14	0.96	0.45	-1.27	-5.78
5	5.11		-0.07	-0.89	-0.21	0.93	0.45	-1.29	-5.59
12	7.91		-0.10	-0.82	-0.30	0.91	0.23	-2.10	-5.16
24	11.19		-0.10	-0.89	-0.41	0.96	0.23	-2.08	-5.87
48	15.82		-0.12	-0.90	-0.42	0.92	0.10	-2.23	-5.84
72	19.38		-0.13	-0.92	-0.50	0.94	0.11	-2.24	-5.89

*Soil properties:
Volumetric heat capacity = 1.007 cal/cm³ °C
Thermal conductivity = 16.05 cal/cm h °C
Latent heat of fusion = 28.96 cal/cm³

Initial conditions:
Semi-infinite body isothermal at 0°C
Boundary condition:
Temperature = -5°C at surface for time > 0

freezing of the uppermost element. One factor contributing to the inaccuracy of the FEM solution is that the forced upper boundary conditions do not precisely represent the analytical problem. The analytical problem is one where the semi-infinite body is initially at uniform temperature and for succeeding times a different temperature is applied at the upper surface. In contrast, the FEM solutions can only approximate this step change, because a smooth gradient, defined by the shape function, exists between the temperature at the surface node and that at the other boundary node of the uppermost element. The freezing algorithm requires repeated application of this approximation if the element takes more than one time increment to freeze.

Despite some error near the top of the profile, differences of only a few percent generally occur after several hours of simulation. Similar studies were conducted using second order shape functions, and behavior with respect to various combinations of the time and depth increments was similar; the accuracies of the solutions were not significantly improved over those obtained with linear shape functions.

Moisture Flux

There are no known analytical solutions for the Richard's equation for unfrozen or freezing soils. Therefore, to verify the finite element representation of the equation, above-freezing isothermal conditions were imposed and comparisons were made with an approximate solution suggested by Philip (1957) and detailed by Kirkham and Powers (1972). Guymon and Luthin (1974) state that rough computations by Philip's method using the same soil-water parameters indicate that the wetting curves in their report were "approximately correct." Two of the curves from Guymon and Luthin (1974) are shown in Figure 6 as are two curves from the present computer model. Agreement between the two models is very good, and data from these and other simulations indicate that the computer model for moisture flux under isothermal conditions approximates the test solution reasonably well. It was also concluded that the finite element solution was not particularly sensitive to parameter update frequency or element length.

Several test solutions were conducted to determine the sensitivity of the finite element model to parameter errors. Parameters evaluated included hydraulic conductivity, porosity and Gardner's constants A_k and A_w. Results, which were developed from an early version of the model using linear shape factors, are shown in Figure 7. The ordinate in Figure 7 is the average difference in computed pressures for the "base" case and the altered case. The average pressure is determined from the pressures at depths of 10, 20, 30 and 40 cm. The data indicate that solution accuracy is highly dependent on the hydraulic conductivity and porosity. Data also indicate that a change in the hydraulic conductivity has the opposite effect of a change in the porosity and that changes in A_w and A_k also have opposing effects. Additional discussion on the effect of Gardner's coefficients and the hydraulic conductivity is in *Frost Heave of Homogeneous Laboratory Samples*.

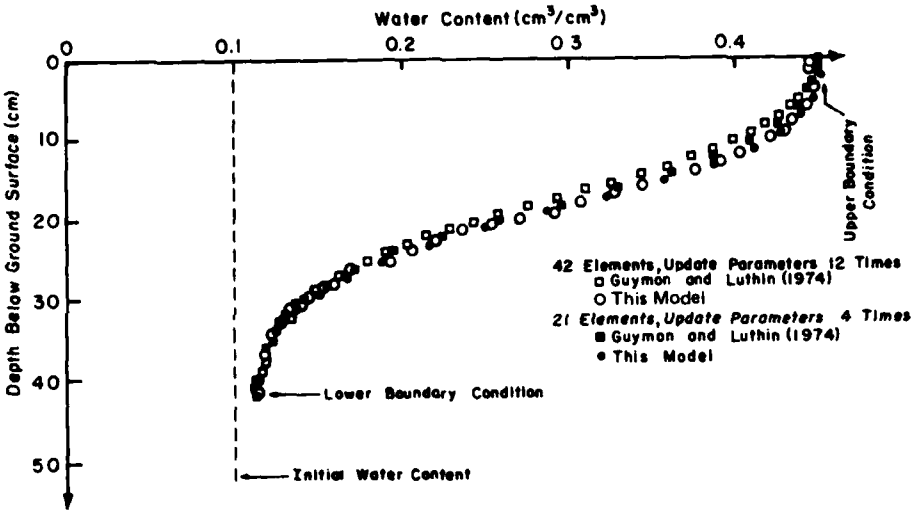

Figure 6. Comparison of FEM solutions of Richard's equation.

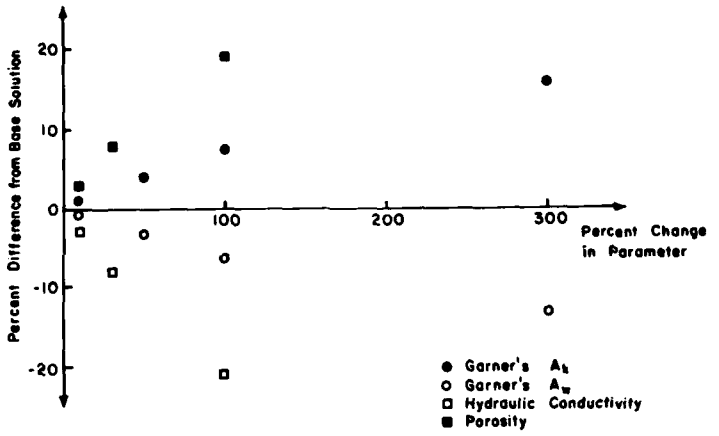

Figure 7. Sensitivity of parameter errors.

Numerical Dispersion

The heat flow and moisture flow equations are based on the assumption that the primary flux is by conduction of heat and moisture. Significant numerical dispersion may be introduced into the solutions of these nonsymmetrical equations if convective effects dominate or are overly significant. In the case of Richard's equation, these effects are determined by the dimensionless ratio, $K^* \Delta x/K$, where K is the unsaturated hydraulic conductivity, K^* is defined by eq 6a, and Δx is the element length. If this ratio reaches a value near unity, numerical dispersion may become significant. For most actual conditions, it is not anticipated that numerical dispersion caused by convective effects will be a problem. However, in our sensitivity studies this ratio did at times reach a critical state at one or more nodal points. The ratio was calculated for each nodal point at each time step and if the ratio reached or exceeded unity the computer solution was terminated.

For the heat flux equation, the appropriate critical ratio is $C_w V \Delta x/K_T$ where C_w is the volumetric heat capacity of water, V the velocity flux, and K_T the thermal conductivity. As in the moisture flux equation, numerical dispersion may become significant if the ratio approaches unity. This ratio is also computed at each nodal point at each time increment. If the ratio reaches or exceeds unity, the solution is terminated.

For a typical soil, C_w equals about 1 cal/cm^3 °C and $K_T = 5.0 \times 10^{-3}$ cal/cm s °C. An element length of 2 cm is typical in model trials. If unity is taken as the critical

Table 4. Comparison of calculated and experimental frost penetration and frost heave.

All frost depths are from the original surface. Soil is New Hampshire silt with an initial density of 1.73 g cm^{-3} and an initial moisture content of 31.3% by volume.

			Calculated results									
			$\Delta t = 1.0\ h$, $A_k = 7.0\times10^{-6}\ cm^{-3}$, $K_{31.3} = 1.83\times10^{-4}\ cm/h$		$\Delta t = 1.0\ h$, $A_k = 7.0\times10^{-7}\ cm^{-3}$, $K_{31.3} = 1.7\times10^{-3}\ cm/h$		$\Delta t = 0.75\ h$, $A_k = 7.0\times10^{-7}\ cm^{-3}$, $K_{31.3} = 1.75\times10^{-3}\ cm/h$					
Experimental Results			*Convection in both equations (Simulation 1)*		*Convection in both equations (Simulation 2)*		*Convection in both equations (Simulation 3)*		*No heat transfer by convection (Simulation 4)*		*Neither heat nor mass transfer by convection (Simulation 5)*	
Elapsed time (days)	*Frost depth (cm)*	*Frost heave (cm)*	*Frost depth (cm)*	*Frost heave (cm)*	*Frost depth (cm)*	*Frost heave (cm)*	*Frost depth (cm)*	*Frost heave (cm)*	*Frost depth (cm)*	*Frost heave (cm)*	*Frost depth (cm)*	*Frost heave (cm)*
1.0	2.1	0.6	6.0	0.3	6.0	0.5	6.0	0.6	6.0	.6	6.0	.6
2.0	–	–	8.2	0.5	8.0	0.9	8.6	1.0	8.6	1.0	8.2	1.1
3.0	6.1	1.3	10.8	0.6	10.0	1.3	10.0	1.6	10.0	1.6	10.0	1.6
4.0	7.1	1.5	11.6	0.9	10.0	2.1	12.0	2.0	12.0	2.0	10.0	2.5
5.0	7.7	1.7	13.7	0.9	10.0	3.0	12.0	2.8	12.0	2.9	10.0	3.6

ratio, then a velocity of 2.5×10^{-3} cm/s is critical. Silts and slightly coarser-grained soils may have saturated hydraulic conductivity (permeability) values in this range. This ratio is also computed for each nodal point at each time step. If the ratio reaches or exceeds unity, the computer solution is terminated. Guymon and Hrodmadka (in prep.) are studying a slightly different formulation which virtually eliminates this problem.

Frost Heave of Homogeneous Laboratory Samples

Initial solutions to problems with arbitrarily chosen initial and boundary conditions indicated that the frost heave algorithm behaved well qualitatively. Therefore, comparison was made between frost depths and frost heave computed by the model and values measured in controlled laboratory experiments. The measured data were from a standard CRREL frost-susceptibility test on Manchester silt (generally called New Hampshire silt in the literature). Initial conditions for the model were measured conditions at the beginning of the test, and the time dependent temperature boundary conditions for the model were those measured during the test.

Since unsaturated hydraulic conductivities at different moisture contents had not been measured for New Hampshire silt, the value of A_k (used in Gardner's relationship) was estimated. Accuracy of the estimate was determined from a comparison of calculated and experimental frost heave and frost penetration. Table 4 contains a comparison of experimental and calculated results. The same spatial discretization, 2-cm element length, was used for all simulations in Table 4.

Comparison of simulations 1 and 2 shows the effect of changing Gardner's soil permeability coefficient A_k. The saturated hydraulic conductivity (permeability) of this soil was 4.0×10^{-2} cm/h at a porosity of 36.2%. Using these data in eq 4, hydraulic conductivities of 1.83×10^{-4} cm/h at a moisture content of 31.3% by volume (300 cm of water tension) and of 6.65×10^{-6} cm/h at a moisture content of 6.8% by volume (950 cm of water tension) are computed. The value of A_k used in simulations 2–5 corresponded to a hydraulic conductivity of 1.75×10^{-3} cm/h at the 31.3% moisture content and to 6.64×10^{-5} cm/h at the 6.8% moisture content. Therefore, between simulation 1 and 2 unsaturated hydraulic conductivities differ by roughly an order of magnitude. In simulation 1, the lower hydraulic conductivities resulted in the complete cessation of heave after four days (while the freezing front advanced steadily); in simulation 2, a massive ice lens grew after three days and the freezing front ceased to advance because the rate of heat extraction was just adequate to freeze the inflowing moisture.

Comparison of simulations 2 and 3 illustrates the effect of time discretization. In going from one time increment size to another, the rate of freezing is only slightly altered in the second day of simulation. However, when the rate of heat extraction is slow and water influx

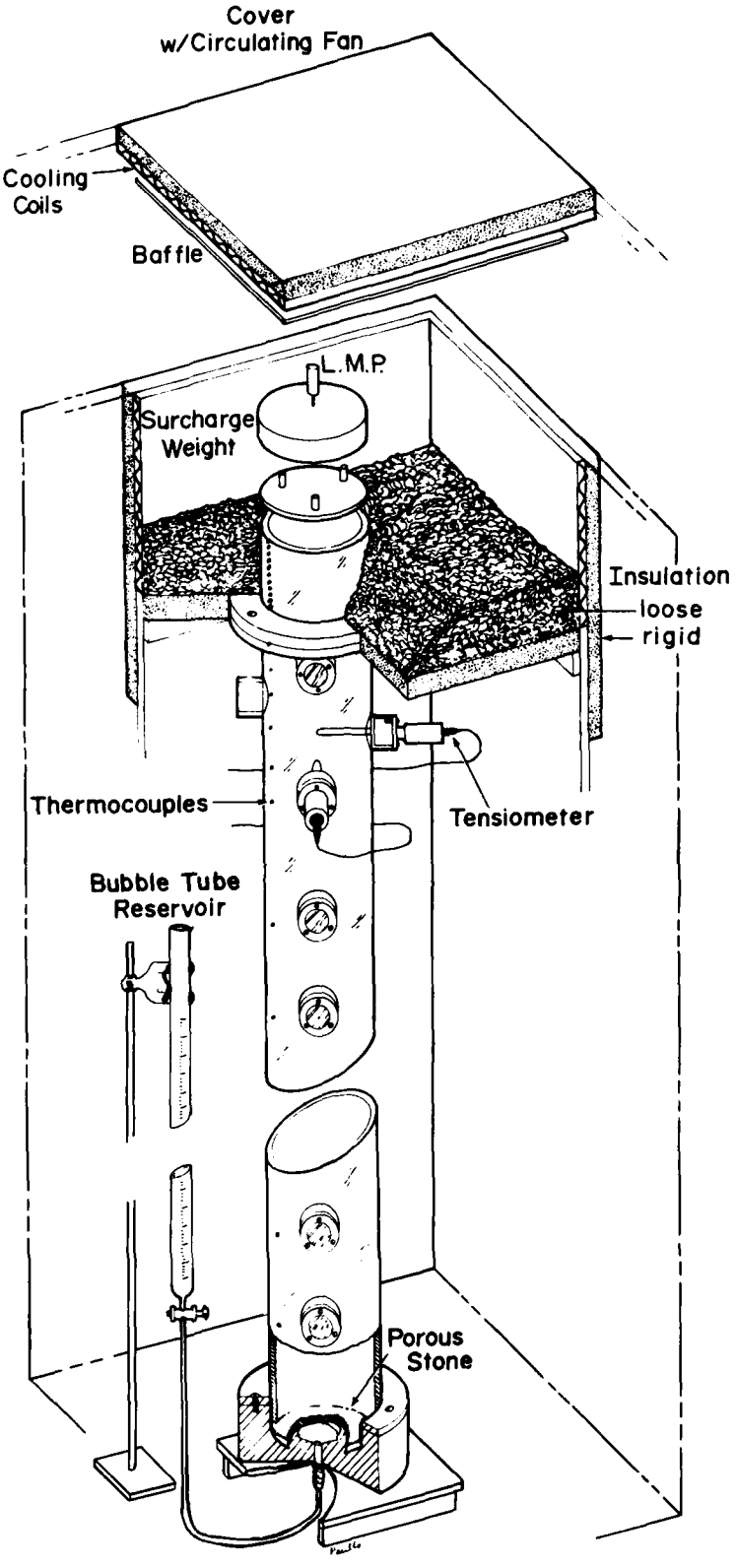

Figure 8. Test cylinder to evaluate effects of surcharge on frost heaving.

is significant, the freezing rate is strongly coupled with the existing spatial discretization, so that relatively large differences exist between the two simulations for days 4 and 5.

Simulations 3, 4 and 5 illustrate the magnitude of the contribution of the convective terms. By eliminating the convective contribution to heat transport (simulation 4) we see, at most, only a small change in calculated temperatures, frost depths, and the amount of heave. Elimination of the convection term in the moisture flow equation (simulation 5) has a slightly larger effect on the first few days of simulated results and a dramatic effect of misleading magnitude on the results beginning with day 4, which were dominated by the influence of spatial discretization. The early days of simulation show slower frost penetration and greater frost heaving in simulation 5 than in simulation 4 because the convective mass transport term includes the effect of gravity; its elimination allows more water to be drawn to the freezing front.

A test cylinder (Fig. 8) was constructed to develop data to provide a preliminary verification of the overburden and/or surcharge portion of the frost heave algorithm. The test cylinder was about 1 m long× 15-cm inside diameter. The upper 15 cm of the cylinder was placed inside a freezing cabinet. It is removable from the lower portion. Loose insulation was placed around the upper 15 cm segment and only the upper surface was exposed to freezing temperatures, thus allowing one-dimensional heat flux from the upper portion of the cylinder. Tensiometers and thermocouples were installed within the soil to measure soil water tension and temperatures, respectively. A "bubble tube" reservoir was used to control the free-water level in the sample.

Berg et al. (in prep.) discuss the test cylinder and results from three tests which were conducted with the cylinder. Figures 9 and 10 show results from two tests in which a surcharge equivalent to 35 cm of water was used. Fairbanks silt compacted to a density of approximately 1.55 g/cm^3 was used in all tests. Samples were placed and compacted slightly below the optimum moisture content. Prior to initiating freezing, the water table was raised to the surface of the sample until free water appeared. It was then lowered to a depth of 45 cm for several days prior to freezing. It was held at the 45-cm depth during the test.

Since the initial temperature and moisture conditions were similar in both tests, a series of computer simulations were made and compared with measured data after 10 days of freezing; results are shown in Table 5. Various combinations of three parameters affecting the quantity of moisture flux and thus the magnitude of frost heaving were used in the simulations. The three parameters varied were Gardner's hydraulic conductivity coefficient A_k Gardner's moisture coefficient A_w and the permeability or saturated hydraulic conductivity (eq 4-7).

Simulation 1 used values for the three parameters which were measured on samples of Fairbanks silt at approximately the same density as the samples in the freezing tests. With these values neither the frost depth nor the amount of frost heave was accurately computed. Several additional simulations were made by changing the value of one or more parameters.

In simulations 2-7, only one parameter per simulation differed from values used in simulation 1. In simulations 8-16, more than one of the parameters were varied in each trial. Results from simulations 4 and 7 indicate that increasing the permeability enhanced both the frost depth and the frost heave after 10 days. The amount of frost heave, however, was only about one-third of that observed in the laboratory tests. Results from simulation 15 agreed most closely with measured values of frost heave, but computed and measured frost penetration depths do not agree as well as in some other trials.

Figure 11 illustrates computed and measured values of frost heave and frost penetration as functions of time. Frost heave is computed reasonably well throughout the entire duration of the test. The upper set of "calculated" frost depth points represents the lower limit of the solidly frozen zone; i.e. computed temperatures above this level are below the freezing point depression temperature (-0.1°C) in the simulations for this soil or, stated in another way, sufficient excess degrees (eq 27) have been accumulated to freeze the soil to this depth. The lower set of "calculated" frost depth points forms the lower limit of the 0°C isotherm. In other words, the area between the two sets of "computed" frost depth points is a freezing zone as determined by the model. Calculated temperatures in the freezing zone are between 0°C and -0.1°C.

Electrical resistivity gages (Atkins 1976) were installed in the sample used in test 2. These devices operate on the principle that the electrical resistivity of ice is much greater than that of water. In test 2, copper wires were flattened and installed 1 cm below the sample surface and at 2-cm intervals to a depth of 15 cm. By measuring the electrical resistance between each pair of electrodes and plotting the data as a function of time, it was possible to determine the time when about one-half of the soil moisture was frozen and the time when most of the remaining moisture froze. (This soil has a significant amount of unfrozen water at sub-freezing temperatures near 0°C, according to Anderson and Tice 1972.) Figure 12 contains plots of the 0°C isotherm vs time as well as lines showing when approximately 50% and 100% of the soil water was frozen at various depths.

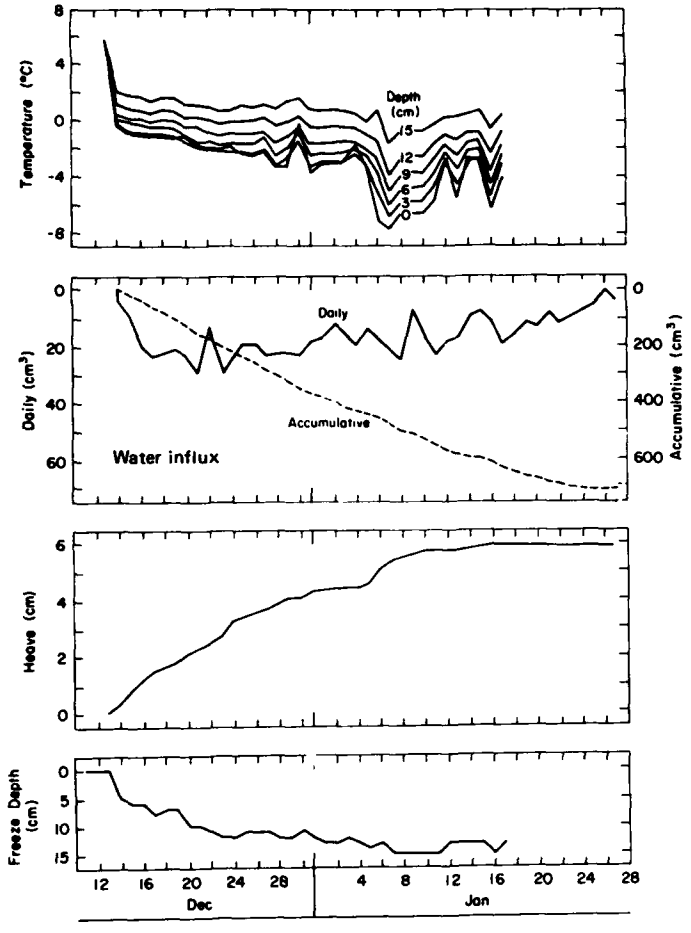

a. *Temperatures, water absorption, frost heave and frost depth plots.*

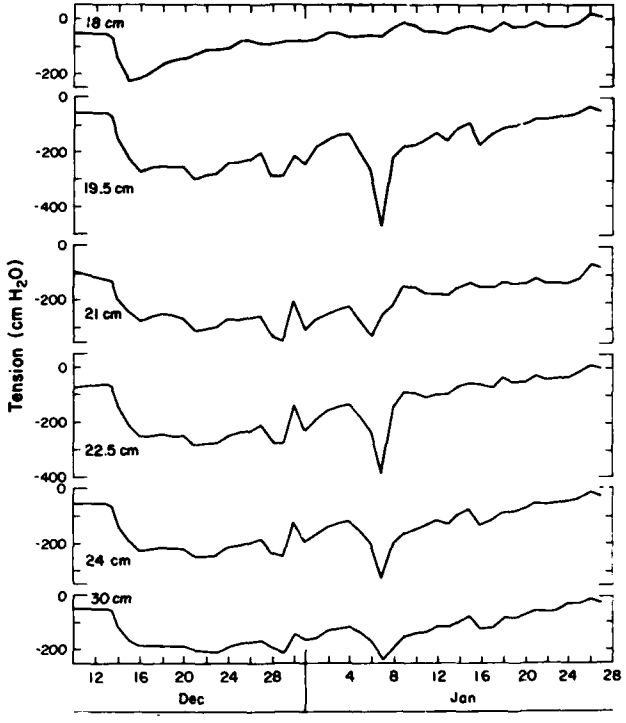

b. *Soil moisture stress at various depths.*

Figure 9. Results from test 1 on Fairbanks silt with surcharge equivalent to 35 cm of water.

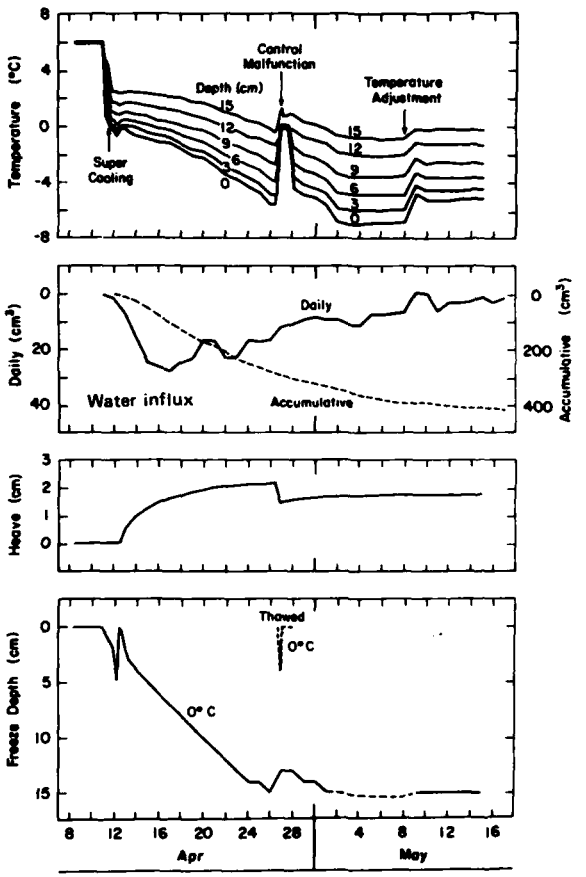

a. Temperatures, water absorption, frost heave and frost depth plots.

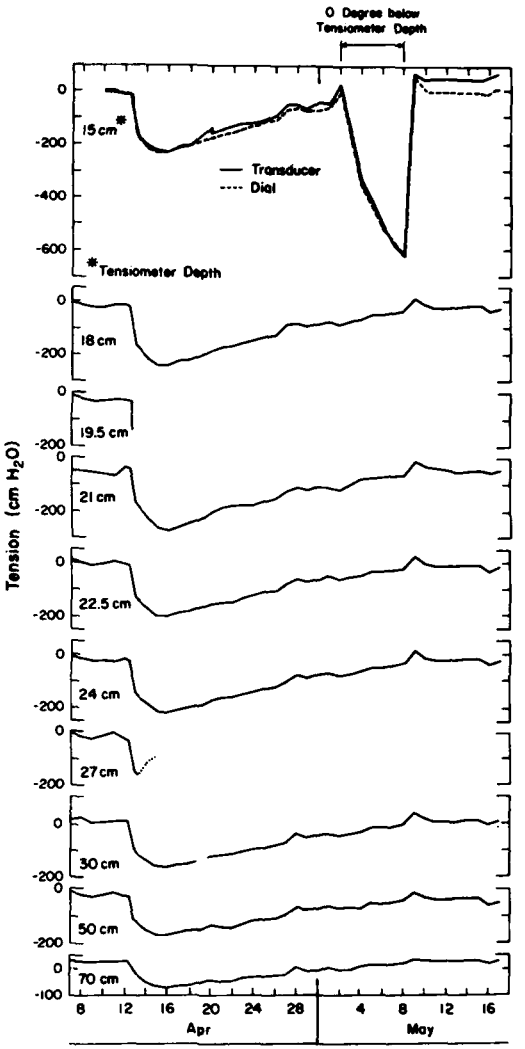

b. Soil moisture stress at various depths.

Figure 10. Results from test 2 on Fairbanks silt with surcharge equivalent to 35 cm of water.

Table 5. Frost penetration and frost heave after 10 days of laboratory freezing.

Simulation	A_k*	A_w†	*Permeability (cm/h)*	*Frost depth (cm)*	*Frost heave (cm)*
1	5E-5**	3E-9	5E-5	9.69	0.06
2	5E-4	3E-9	5E-5	9.39	0.00
3	5E-5	3E-8	5E-5	10.00	0.15
4	5E-5	3E-9	5E-4	10.00	0.33
5	5E-5	3E-7	5E-5	11.20	0.09
6	5E-6	3E-9	5E-5	9.98	0.17
7	5E-5	3E-9	5E-3	10.50	0.66
8	5E-4	3E-9	5E-3	10.00	0.35
9	5E-3	3E-9	5E-3	9.69	0.06
10	5E-4	3E-10	5E-3	7.78	0.00
12	5E-6	3E-9	5E-3	9.99	1.24
13	5E-5	3E-8	5E-3	10.30	0.98
14	5E-6	3E-8	5E-3	10.50	0.89
15	5E-6	3E-9	5E-2	8.5	2.28
16	5E-6	3E-9	1.1E-1	7.9	3.69
–	Laboratory test 1			12.0	2.75
–	Laboratory test 2			12.5	2.05

*Gardner's hydraulic conductivity coefficient.
†Gardner's moisture coefficient.
**5E-5 = 5×10^{-5} etc.

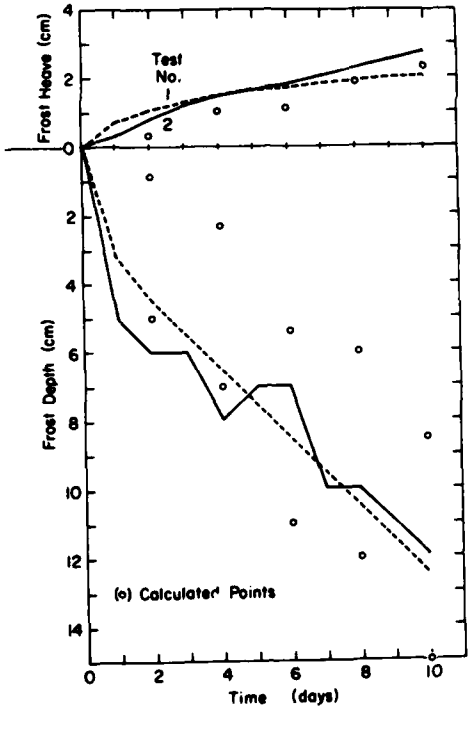

Figure 11. Computed and measured frost heave and frost penetration on Fairbanks silt with surcharge of 35 cm of water.

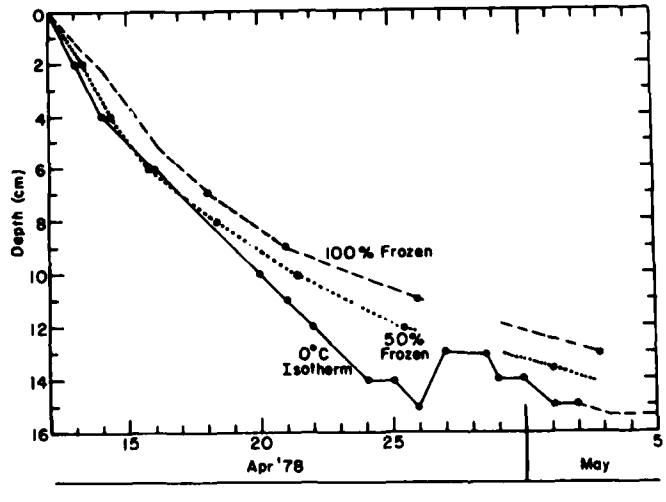

Figure 12. Temperature and electrical resistivity gage data for test 2.

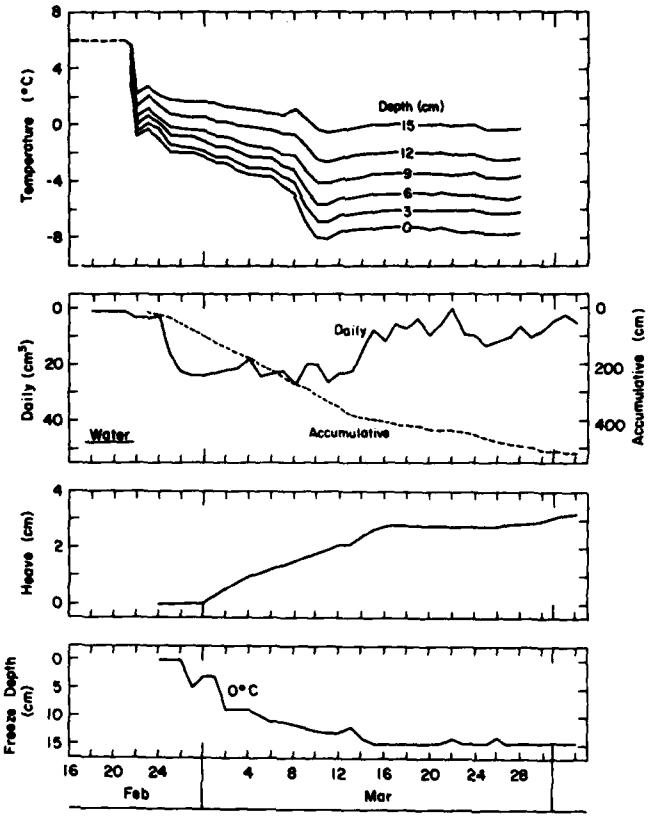

a. Temperatures, water absorption, frost heave and frost depth plots.

Figure 13. Results from test 3 on Fairbanks silt with surcharge equivalent to 350 cm of water.

The freezing zone, i.e. the distance between the 0°C isotherm and the solidly frozen line, is not nearly as wide as the computed freezing zone in Figure 11. The width of the zone is not constant, but increases with time. Until the solidly frozen soil penetrated to a depth at about 7 cm, it corresponded to a temperature of about -0.3°C; thereafter the boundary of the solidly frozen soil corresponded with progressively lower temperatures. On 3 May the solidly frozen boundary was at 13 cm which conformed to a temperature of -2.2°C. An unintentional, partial freeze-thaw cycle occurred on 26 April (Fig. 11) when the sample thawed to a depth of about 5 cm and the remainder of it warmed substantially. Whether this cycle affected the amount of unfrozen water when it was refrozen is unknown at this time.

Data from tests 1 and 2 and from the computer simulations in Table 5 indicate that the model can accurately predict the amount of frost heave and frost penetration in short-duration laboratory samples. Data from Table 5 again illustrate, however, that heave and frost penetration are quite sensitive to the hydraulic properties used in the solutions.

A third test was conducted in this series to determine the validity of eq 32. A surcharge equivalent to a pressure of 350 cm of water was applied to the soil column prior to initiation of freezing. If eq 32 adequately represented effects of overburden and surcharge, the soil water tension measurements would have been lower, i.e. less negative, during this test than during the previous two tests.

Figure 13, which contains data observed during the third test, shows that the measured soil water tension values are not significantly different from those meas-

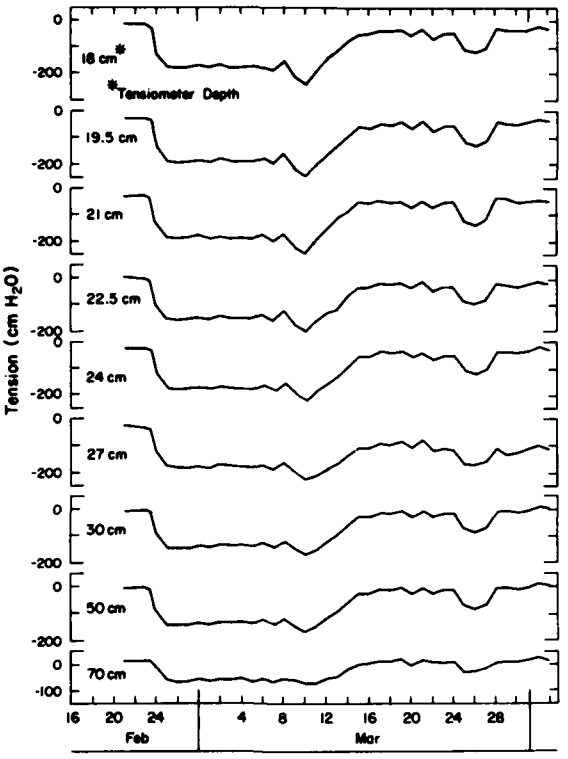

b. Soil moisture stress at various depths.

Figure 13. (cont'd)

ured in the other two tests with a surcharge pressure of 35 cm of water (Fig. 9 and 10). Data from Figure 10 indicated that the maximum soil water tension observed as the freezing front approached a tensiometer at a depth of 15 cm was about -650 cm of water. Using this value of P_w in eq 32 we calculate P_c = -1622 cm of water for test 2. If we assume P_c does not change due to the added surcharge, we anticipate that a maximum tensiometer reading of about -490 cm of water will occur at the freezing front in test 3. Unfortunately, a tensiometer was not located in the freezing zone in test 3, but tensions at the 18-cm depth and below did not show a significant change from test 2. These results do not completely eliminate the possibility that eq 32 is valid, however, because soil moisture tension data were not measured in the immediate vicinity of the freezing zone in all three tests. It is possible that significant changes in tension values in this area were not reflected in pressure gradients a few centimeters away.

Berg et al. (in prep.) present a thorough discussion of results from all three tests which were conducted in this series.

CONCLUSIONS

A one-dimensional mathematical model coupling simultaneous heat and moisture fluxes in freezing soil-water systems has been developed. The finite element method was used to solve the problem, and others (e.g. Taylor and Luthin 1976 and 1978, Harlan 1972 and 1973, Dempsey 1978 and Outcalt 1976) have solved the one-dimensional coupled heat and moisture flow equations using finite difference procedures.

This model has successfully been used to simulate frost penetration and frost heave which were observed in relatively homogeneous laboratory test specimens.

The amount of water flux, and resultant frost heave, computed from the model, is very sensitive to the hydraulic properties of the soil. This agrees qualitatively with field observations; i.e. certain soils, such as silts, have optimum hydraulic properties to cause severe frost heave.

A work plan was developed for correlating results of various laboratory test methods for assessing frost heave susceptibility of soils and the amount of heave observed

at field study sites. This mathematical model can be used to help correlate the field and laboratory data. Appendix A contains the work plan.

Field instrumentation necessary for correlating laboratory and field observations of frost heave would be nearly the same as that required for investigations of the thaw-weakening of subgrade soils and granular unbound base courses. A proposed investigational procedure for laboratory and field studies related to thaw weakening is presented in Appendix B.

Possibly the most important, but as yet unsubstantiated, application of the mathematical model is to predict the amount of frost heave which may occur in a given pavement system at a given geographical location. Since it is based entirely upon principles of heat and moisture flux, the model does not require, or use, data from any of the laboratory frost-susceptibility test methods. If the mathematical model can be used to estimate the likely range of frost heave of candidate pavement profiles, we have made a significant improvement in the procedure for designing roadway and airfield pavements in seasonal frost areas.

RECOMMENDED STUDIES TO REFINE THE MODEL

In September 1978, the Corps of Engineers, the Federal Highway Administration and the Federal Aviation Administration commenced a study to correlate laboratory and field measurements of frost-susceptibility and frost heave and laboratory and field studies of the extent and duration of thaw weakening. The model developed in the present study will be refined and applied in the recently initiated study.

Necessary refinements to the mathematical model can be divided into two broad categories: 1) to improve computational efficiency and 2) to improve the accuracy of estimates of frost penetration and frost heave. Improvements in the computational efficiency should include more efficient storage of data within the matrices, less time-consuming manipulation of the matrices and improved formulation of certain aspects of the problem to allow using smaller computers or decreasing solution times.

Improving the accuracy of estimating frost penetration and frost heave requires a more complete understanding and/or representation of thermal, hydrological and mechanical processes within the freezing zone. Specifically, algorithms which incorporate the effects of surcharge and overburden are necessary. Expressions for the relationships between soil moisture tension and moisture content and soil moisture tension and unsaturated hydraulic conductivity are used in the computations. We must develop expressions which suitably relate these parameters, and it may also be necessary to incorporate effects of hysteresis on these parameters. In the recently initiated joint study it is planned to construct a dual gamma beam device which can nondestructively scan through a soil column similar to the one shown in Figure 8. This device will permit simultaneous measurement of changes in moisture content and density as the soil column freezes. In addition, relationships between soil moisture tension and moisture content and between soil moisture tension and unsaturated hydraulic conductivity can be determined directly from data obtained with the soil column instrumentation and the dual gamma system.

Laboratory tests involving freeze-thaw cycles and layered soil systems may be required to more thoroughly validate the model prior to predicting frost penetration and frost heave from actual road and airfield pavements. These more complex problems have not been addressed in the current study, and although no major problems are anticipated when extending the model to these conditions, minor complications will inevitably arise.

The final test of the model will be to predict frost heave and frost penetration of instrumented field test sections. If the model passes these tests, it can confidently be applied to assessing frost heave in various pavement profiles under various environmental conditions.

This one-dimensional model cannot be used to predict differential frost heave. Perhaps the model should be used in conjunction with another model, which may be statistically based, which describes spatial variations of the important parameters. This problem will be studied during the recently initiated studies.

LITERATURE CITED

Aitchison, G.D., ed. (1965) *Moisture equilibria and moisture changes in soils beneath covered areas: A symposium in print*. Sydney, Australia: Butterworth and Company Ltd.

Anderson, D.M. and A.R. Tice (1972) Predicting unfrozen water contents in frozen soils from surface area measurements. *Highway Research Board Bulletin 393*, p 12-18.

Anderson, D.M., A.R. Tice and H.L. McKim (1973) The unfrozen water and the apparent specific heat capacity of frozen soils. *Permafrost: Second International Conference*, National Academy of Sciences.

Atkins, R.T. (1979) Determination of frost penetration by soil resistivity measurements. CRREL Special Report 79-22.

Bafus, G.R. and G.L. Guymon (1976) Thermal analysis of frozen embankment islands. *Journal of Waterways, Harbors and Coastal Engineering Division, ASCE*, vol. 102, no. WW2, p. 123-139.

Barker, W.R. and W.N. Brabston (1975) Development of a structural design procedure for flexible airport pavement. U.S. Army WES Report S-75-17.

Berg, R.L. (1976) Thermoinsulating media within embankments on perennially frozen soil. CRREL Special Report 76-3, AD 062 442.

Berg, R.L., J. Ingersoll and G.L. Guymon (In prep.) Heat and moisture transfer in Fairbanks silt during open system freezing. Prepared for presentation at the Third Conference on Soil-Water Problems in Cold Regions, Calgary, Alberta.

Berg, R.L. and T.C. Johnson (1976) Development of a mathematical model to correlate observed frost heave of highway and airport pavements with laboratory predictions. Interim report (unpublished) to FHWA and FAA by CRREL on purchase order 5-3-0202.

Bergan, A.T. and C.L. Monismith (1972) Some fatigue considerations in the design of asphalt concrete pavements. Proceedings, Canadian Technical Asphalt Association, vol. XVII.

Beskow, G. (1935) Soil freezing and frost heaving with special application to roads and railroads. Translated by J.O. Osterberg, Technical Institute, Northwestern University.

Bird, R.B., W.E. Stewart and E.N. Lightfoot (1960) *Transport phenomena*. John Wiley and Sons: New York.

Cary, J.W. and H.F. Mayland (1972) Salt and water movement in unsaturated frozen soil. *Soil Science Society of America, Proceedings*, vol. 32, p. 549-555.

Christison, J.T. (1972) The response of asphaltic concrete pavements to low temperatures. PhD. thesis (unpublished), Department of Civil Engineering, University of Alberta, Edmonton, Alberta.

Dempsey, B.J. (1969) A heat-transfer model for evaluating frost action and temperature related effects in multilayered pavement systems. PhD. thesis (unpublished), Department of Civil Engineering, University of Illinois, Urbana, Illinois.

Dempsey, B.J. (1976) Climatic effects of airport pavement systems: State of the art. USAE WES Contract Report S-76-12.

Dempsey, B.J. (1978) A mathematical model for predicting coupled heat and water movement in unsaturated soil. *International Journal for Numerical and Analytical Methods in Geomechanics*, vol. 2, p. 19-34.

DeVries, D.A. (1952) The thermal conductivity of soil. *Meded, Landbouwhogesch. Waneningen.* vol. 32, p 1-72.

DeVries, D.A. (1966) Thermal properties of soils. In *Physics of Plant Environment* (W.E. Van Wijk, ed.) North-Holland Publishing Co., Amsterdam, p 210-135.

Dirksen, C. (1964) Water movement and frost heaving in unsaturated soil without an external source of water. PhD. thesis (unpublished), Cornell University.

Dirksen, C and R.D. Miller (1966) Closed-system freezing of unsaturated soil. *Soil Science Society of America, Proceedings*, vol. 30, p 168-173.

Dusinberre, G.M. (1961) *Heat transfer calculations by finite differences*. Scranton, Pennsylvania: International Textbook Company.

Edelfson, N.E. and A.B.C. Anderson (1943) Thermodynamics of soil moisture. *Hilgardia*, vol. 15, no. 2.

Everett, D.H. (1961) The thermodynamics of frost action in porous solids. *Transactions of the Faraday Society*, vol. 57, p 1541-1551.

Fredlund, D.G.; A.T. Bergan and E.K. Sauer (1975) Deformational characterization of subgrade soils for highways and runways in northern environments. *Canadian Geotechnical Journal*, vol. 12, p 213.

Gardner, W.R. (1958) Some steady-state solutions of the unsaturated flow equation with application to evaporation from a water table. *Soil Science*, vol. 88, p 228-232.

Gold, L. (1957) A possible force mechanism associated with the freezing of water in porous materials. Highway Research Board Bulletin 168, National Research Council, Washington, DC.

Guymon, G.L. (1976) Finite element analog of frost heave. Final report on CRREL Contract DACA 89-76-G-055 (unpublished).

Guymon, G.L. and T.V. Hromadka (In prep.) Numerical problems involved with modeling heat and mass transfer. CRREL Special Report.

Guymon, G.L. and J.L. Luthin (1974) A coupled heat and moisture transport model for Arctic soils. *Water Resources Research*, vol. 10, no. 5, p 995-1001.

Harlan, R.L. (1972) Ground conditioning and the groundwater response to winter conditions. *Proceedings, International Symposia on the Role of Snow and Ice in Hydrology, Symposium on Properties and processes*, Banff, Alberta.

Harlan, R.L. (1973) Analysis of coupled heat-fluid transport in partially frozen soil. *Water Resources Research*, vol. 9, no. 5, p 1314-1323.

Hoekstra, P. (1966) Moisture movement in soils under temperature gradients with the cold-side temperature below freezing. *Water Resources Research*, vol. 2, no. 2, p 241-250.

Hoekstra, P., E. Chamberlain and A. Frate (1965) Frost-heaving pressures. CRREL Research Report 176, AD 626 175.

Hromadka, T.V. and G.L. Guymon (in prep.) The latent heat problem associated with numerical models of freezing soils. Submitted to *Water Resources Research*.

Jame, Y.W. (1978) Heat and mass transfer in freezing unsaturated soil. PhD. thesis (unpublished), University of Saskatchewan, Saskatoon, Saskatchewan.

Jame, Y.W. and D.I. Norum (1972) Phase composition of a partially frozen soil. Research Paper no. 11, Division of Hydrology, College of Engineering, University of Saskatchewan, Saskatoon, Saskatchewan.

Jame, Y.W. and D.I. Norum (1976) Heat and mass transfer in freezing unsaturated soil in a closed system. *Proceedings, Second Conference on Soil Water Problems in Cold Regions*, Edmonton, Alberta.

Johansen, O. (1977) Frost penetration and ice accumulation in soils. *Proceedings, Frost Action in soils*, University of Lulea, Lulea, Sweden.

Johnson, A.W. (1952) Frost action in roads and airfields. Special Report 1, Highway Research Board, National Research Council, Washington, DC.

Johnson, A.W. and C.W. Lovell, Jr. (1953) Frost action research needs. Highway Research Board Bulletin 71, National Research Council, Washington, DC.

Johnson, T.C., R.L. Berg, K.L. Carey, and C.W. Kaplar (1975) Roadway design in seasonal frost areas, CRREL Technical Report 259, and TRB Synthesis of Highway Practice No. 26.

Jumikis, A.R. (1966) *Thermal soil mechanics*. New Brunswick, New Jersey: Rutgers University Press.

Kersten, M.S. (1949) Laboratory research for determination of the thermal properties of soils. ACFEL Technical Report 23, AD 712 516.

Keune, R. and P. Hoekstra (1967) Calculating the amount of unfrozen water in frozen ground from moisture characteristic curves. CRREL Special Report 114, AD 659781.

Kinosita, S. (1975) Soil-water movement and heat flux in freezing ground. *Proceedings, First Conference on Soil-Water Problems in Cold Regions*, Calgary, Alberta.

Kirkham, D. and W.L. Powers (1972) *Advanced soil physics*. New York: John Wiley and Sons, Inc.

Loch, J.P. and B.D. Kay (1978) Water redistribution in partially frozen, saturated silt under several temperature

gradients and overburden loads. *Soil Science Society of America Journal*, vol. 42, no. 3, p. 400-406.

Luikov, A.V. (1966) *Heat and mass transfer in capillary-porous bodies*. Translated by W.B. Harrison, London: Pergamon Press.

Meyers, G.E. (1971) *Analytical methods in conduction heat transfer*. New York: McGraw-Hill.

McGaw, R.W. and A.R. Tice (1976) A simple procedure to calculate the volume of water remaining unfrozen in a freezing soil. *Proceedings, Second Conference on Soil-Water Problems in Cold Regions*, Edmonton, Alberta.

McKim, H.L., R.L. Berg and J. Ingersoll (1976) Development of a remote reading tensiometer/transducer for use in subsurface freezing systems. *Proceedings, Second Conference on Soil-Water Problems in Cold Regions*, Edmonton, Alberta.

McRoberts, E.C. and J.F. Nixon (1975) Some geotechnical observations on the role of surcharge in soil freezing. *Proceedings, First Conference on Soil Water Problems in Cold Regions*, Calgary Alberta.

Miller, R.D. (1978) Frost heaving in non-colloidal soils. *Proceedings, Third International Conference on Permafrost*, Edmonton, Alberta, p. 708-713.

Nielson, D.R., R.D. Jackson, J.W. Cary and D.D. Evans (1972) *Soil water*. American Society of Agronomy and Soil Science Society of America, Madison, Wisconsin.

Organization for Economic Coorperation and Development (1973) *Water in roads: Prediction of moisture content of road subgrades*. OECD, Paris, France.

Outcalt, S. (1976) A numerical model of ice lensing in freezing soils. *Proceedings, Second Conference on Soil-Water Problems in Cold Regions*, Edmonton, Alberta.

Penner, E. (1957) Soil moisture tension and ice segregation. *Highway Research Board Bulletin 168*, p. 50-64.

Penner, E. (1959) The mechanism of frost heaving in soils. *Highway Research Board Bulletin 225*, p. 1-22.

Philip, J.R. (1957) Numerical solutions of equations of the diffusion type with diffusivity concentration dependent. II. *Australian Journal of Physics*, vol. 10, p. 29-42.

Philip, J.R. and D.A. DeVries (1957) Moisture movement in porous materials under temperature gradients. *Transactions, American Geophysical Union*, vol. 38, p. 222-232.

Taber, S. (1930) Freezing and thawing of soils as factors in the destruction of road pavements. *Public Roads*, vol. 11, no. 6, p. 113-132.

Takagi, S. (1978) The adsorption force theory of frost heaving. Presented at the International Symposium on Ground Freezing, Ruhr-University, Bochum, Germany.

Taylor, G.S. and J.N. Luthin (1976) Numerical results of coupled heat-mass flow during freezing and thawing. *Proceedings, Second Conference on Soil Water Problems in Cold Regions*. Edmonton, Alberta.

Taylor, G.S. and J.N. Luthin (1978) A model for coupled heat and moisture transfer during soil freezing. *Canadian Geotechnical Journal*, vol. 15, p. 548-555.

Warren, H.W. and W.L. Dieckmann (1963) Numerical computation of stresses and strains in a multiple-layered asphalt pavement system. Calfornia Research Corporation, Richmond, California.

Williams, P.J. (1967) *Properties and behavior of freezing soils*. Norwegian Geotechnical Institute, Oslo, Norway.

APPENDIX A: WORK PLAN, STAFFING AND INSTRUMENTATION REQUIREMENTS FOR CORRELATING RESULTS OF LABORATORY FROST SUSCEPTIBILITY TESTS WITH FIELD PERFORMANCE

Excerpted from July 1976 Interim Report by R.L. Berg and T.C. Johnson.

INTRODUCTION

In July 1975, the Federal Highway Administration (FHWA), the Federal Aviation Administration (FAA) and CRREL started a jointly funded project to develop a mathematical model of the frost heaving process. The work is being accomplished by CRREL.

Prior to conducting field studies, it was necessary to develop a numerical model for predicting frost heave in roadway and airfield pavements. Otherwise there would have been no effective way to normalize other critical parameters at the various test sites to permit comparative evaluation of the different laboratory methods of determining soil frost-susceptibility. The model will also permit important parameters to be varied separately or simultaneously to assess their influence on frost heaving and should be a valuable analytical tool for use by designers in predicting frost heave.

Development of the mathematical model is the initial step in a broader study which will ultimately involve State Highway Departments, State Departments of Transportation, and airfield construction agencies in a cooperative undertaking to measure frost penetration, frost heave and other important variables in full-scale test sections. When the field tests are conducted, various laboratory methods for assessing the frost susceptibility of the soils will be applied to determine which method gives the most accurate or consistent index for predicting the magnitude of frost heave.

The remainder of this appendix discusses a suggested work plan for the field studies, including the composition of a technical team to conduct the studies, general criteria for site selection, and suggested instrumentation for each test section.

FIELD TEST SITES

The validity of this frost model will be established by full-scale test sections installed at selected locations in several of the northern states. It would be desirable to provide centralized direction for the program by making a single organization responsible for coordinating the overall study, providing assistance on instrumentation and observations, directing and coordinating the related laboratory studies, and interpreting and analyzing results. The organization should have a team of specialists with expertise in the following areas: 1) laboratory soil tests for measurement of frost-susceptibility and of related soil properties, 2) instrumentation for laboratory and field measurement of important thermal and hydrological parameters, 3) collection, storage and management of data from field tests, 4) theories of the frost heaving process, 5) physics and chemistry of soil-water processes, 6) meteorology and computational methods for assessing the surface energy balance on pavement surface, 7) soil mechanics, 8) surface and subsurface drainage of pavement systems, 9) pavement design and construction in seasonal frost areas, and 10) computer programing. In addition, the organization coordinating the study should have the facilities and resources necessary to process the large volumes of data that will be generated from the laboratory and field studies.

Selection of appropriate existing pavements for the field test sections and a suitable choice of instrumentation are critical tasks in the proposed research to assure the highest probability of correlation of data from the various field sites, the laboratory test data, and the mathematical model. To minimize the amount of instrumentation required, and to keep the volume of data generated within manageable limits, it is extremely important that sites be chosen where there is essentially no lateral or longitudinal flow of heat or moisture. Sites of this type would lend themselves to a better simulation by both the laboratory tests and the mathematical model and would require less costly instrumentation and data collection. Table A1 lists factors that should be considered in the site selection process.

Figures A1 and A2 illustrate the observation points and the instrumentation to be installed at a typical test site in a highway pavement. In an airfield pavement the instrumentation would be similar but the test pit could be located 15-20 ft (4.6-6.1 m) from a runway edge. The amount and location of instrumentation are idealized in the two figures, and in a definitive study should be tailored to specific site conditions, availability of equipment and personnel, and funding. These same factors may also strongly influence the type and frequency of observations to be made. Details for instrumentation at a specific site should be developed through discussions between the sponsors, the involved highway or airport operators, and the coordinating organization. The types of instrumentation and observations outlined below are suggested as an optimum system that will provide

Table A1. Considerations in site selection.

1. Little or no transverse slope except crown in pavement.
2. Little or no longitudinal slope.
3. Pavement section not excessively layered, i.e. few materials of widely differing properties.
4. Pavement surface not severely cracked.
5. Stable water table.
6. Occurrence of frost heave of the pavement surface.
7. Pavement kept cleared of snow in winter.
8. Uniform subsurface soil and moisture conditions.
9. Uniform exposure to solar radiation and wind.
10. Minimum of 100-ft-long (30.5 m) pavement segment.
11. Within a reasonable distance of office responsible for observations and servicing of instrumentation.
12. Other factors suggested by the responsible construction agency.

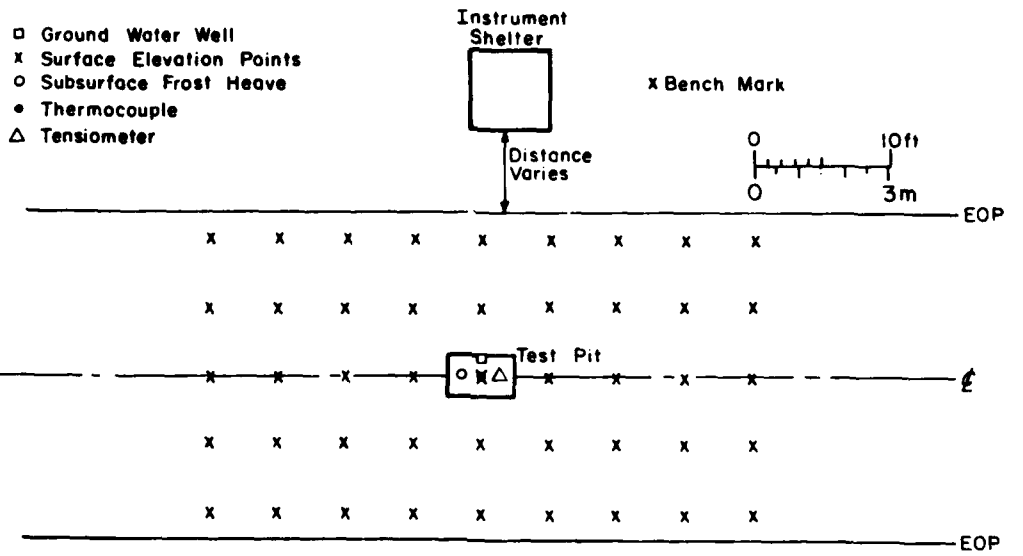

Figure A1. Instrumentation for a typical field site, plan view.

reliable data for correlation between field and laboratory studies. It is recognized that other systems could also be feasible. Forthcoming technological developments may provide less expensive and/or more reliable methods of accomplishing some observations. Table A2 lists the suggested types of instrumentation, the vertical spacing of individual sensors, the frequency of observations and the type of data collection system. Table A3 lists the approximate cost of instrumentation for a typical site. Samples of nearly every material in the pavement profile must be obtained and returned to the coordinating organization for distribution to agencies that will conduct the laboratory tests. Similar soils should be used to replace those removed from the pavements for the laboratory studies.

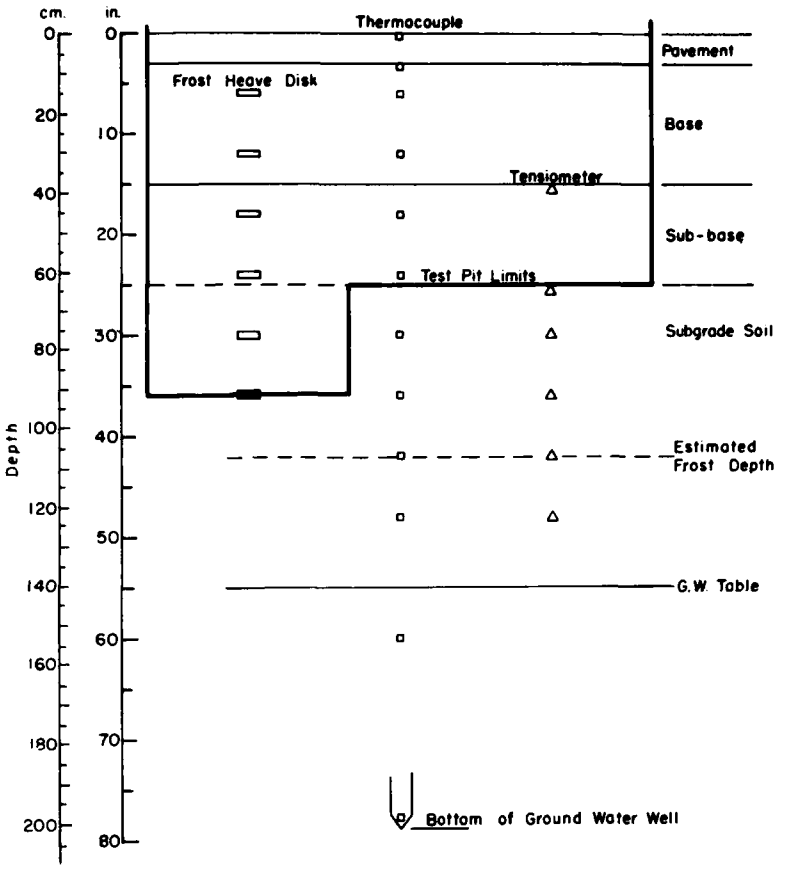

Figure A2. Instrumentation for a typical field site, profile view.

Table A2. Instrumentation for field sites.

Item	*Purpose*	*Observations*	*Spacing*
Thermocouples	Temperatures	Every 6 hours (automatically)	Top and bottom of pavement, every 6 in. (15.2 cm) through frost zone, additional thermocouples 6, 18 and 36 in. (15.2, 45.7 and 91.4 cm) below design seasonal frost depth.
Tensiometers	Stress in soil water	Every 6 hours (automatically)	Every 6 in. (15.2 cm) in fine sands and fine-grained soils in frost zone, one 6 in. below frost zone and one 6 in. below water table.
Frost heave disks	Subsurface frost heave	Daily (automatically)	Every 6 in. (15.2 cm) to a depth of 12 in. (45.7 cm) below subgrade surface.
Groundwater well	Groundwater level	Daily (automatically)	One well, to a depth about 24 in. (61.0) below groundwater table.
Surface elevation points	Frost heave at surface	3 times per week (manually)	Starting from center of test pit, lay out 5X5 ft (1.52X1.52 m) grid for 20 ft (6.1 m) each longitudinal direction and 10 ft (3.05 m) each transverse direction.
Benchmark	Reference point	–	One bench mark which will not be moved by frost heave.
Instrument shelter	House instruments	–	One digital data collection system capable of scanning the desired number of points at the desired intervals. Instrument shelter must maintain 70°±20°F (21.1°±11.1°C) and contain electrical power for data system and other instrumentation and heat and air conditioning systems.

Table A3. Approximate cost of instrumentation at a typical field site.

Thermocouples - 12 sensors		
Wire $0.75/ft X 100 ft ($2.46/m X 30.48 m)	$ 75	
Labor (assembly) 8 h X $10/h	80	
Subtotal		$ 155
Tensiometers - 7 sensors		
Material	$1600	
Labor (assemble, fill and calibrate) 40 h X $10/h	400	
Subtotal		2,000
Frost heave disks - 6 sensors		
Material (6 ea X $20)	$ 120	
Labor (calibration and add extension wire) 16 h X $10/h	160	
Read-out device	2000	
Subtotal		2,280
Groundwater well - 1 sensor		
Material	$ 10	
Labor (fabricate) 4 h X $10/h	40	
Subtotal		50
Surface elevation points	$ 10	
Benchmark	100	
Data system (30 channels)	7000	
Instrument shelter 30 ft^2 (2.79 m^2) @ $30/$ft^2$) ($322.92/m^2)	900	
Test pit (digging and refilling) (16 h X $10/h)	160	
Installing and connecting instrumentation (40 h X $10/h)	400	
Drill rig and operators ($50+8 h X $10/h)	130	
Subtotal		8,700
Total Cost		$13,275

Note that this total does not include indirect costs, overhead costs, monthly costs for power, heat and air conditioning of instrument shelter or labor costs of making observations manually. Nor does it include costs for conducting laboratory frost-susceptibility tests and other laboratory studies and tests. If materials for several test sites were purchased under a single order, discounts on some items could be obtained for quantity lots.

APPENDIX B: PROPOSED INVESTIGATION OF THAW WEAKENING OF SUBGRADE SOIL AND GRANULAR UNBOUND BASE COURSE.

Submitted to the Federal Highway Administration on 13 April 1978.

Most methods of design of pavements whose subgrades are affected by frost action make use of a single index of subgrade supporting capacity. Whether the index be a CBR-value, an R-value, a K-value, a soil support value, a soil classification index, or some other term, it is usual to assign for each soil a single numerical value of the index that is construed to be applicable in design of pavements to serve year-round traffic. The index in some cases is selected to represent the worst case, when the subgrade is severely weakened by thawing, while in other cases it does not account for freezing and thawing and is more representative of the conditions in summer or fall when subgrades have recovered from the thaw-weakened state.

Use of a single index occasions at least two sources of uncertainty. On one hand the design equations, which currently are in almost every case empirical, must include among their coefficients some means of accounting for the extreme seasonal variation in subgrade supporting capacity. And on the other hand, the selected soil index and its numerical values must be able to consistently evaluate a great diversity of soils having markedly different seasonal variations in properties. In view of these uncertainties, it seems hardly surprising that different pavements constructed in frost areas vary from conditions with no evidence of subgrade-related distress (indicating good design or, one might suppose, even overdesign), to those with extensive evidence of subgrade-related distress (indicating underdesign).

As mechanistic design methods (those based on calculated stresses and strains) become more widely adopted, it will be possible to dispel the first uncertainty by incorporating into the method a damage accumulator. The pavement damage that will occur in each season can be calculated and summed to represent the total yearly damage occasioned by traffic. A trial pavement design would then be adopted for construction if the total damage accumulation during the selected number of years of economic life were within limits determined in relation to desired pavement serviceability. Effective application of a cumulative damage approach, however, requires that the actual properties of subgrade soils in each season be determined; accomplishment of this task will also dispel the second uncertainty mentioned above.

Design procedures are available (Bergan and Monismith 1972, Barker and Brabston 1975) for analysis of damage accumulation in pavements subjected to freezing and thawing. Most methods require a prediction of the seasonal values of the resilient modulus of each type of soil, base course, or other material in the pavement profile. While certain information is available (Johnson et al. 1975) regarding effects of frost action on the resilient modulus of soils, further research is needed to develop laboratory test techniques for determining seasonal values of the resilient modulus for design of new pavements and rehabilitation of existing pavements. The resilient properties need to be determined and expressed in relation to pertinent environmental parameters or to soil properties that are sensitive to changes in such environmental conditions. It is expected that the state of stress in the soil moisture will prove to be a convenient parameter, as previous research (Fredlund et al. 1975) has shown that one of the most significant variables affecting the resilient modulus is the moisture tension. Moisture tension has the further powerful advantage that with the recent development of frost-resistant tensiometers (McKim et al. 1976) it can be monitored continuously in situ.

There is currently a critical need for a broad data base of actual values of the resilient modulus for a wide variety of types of subgrade soils and base course materials, measured throughout the year and including periods of freezing, thawing, and recovery. Lack of information on seasonal changes in the resilient modulus constitutes an impediment to the implementation of mechanistic design methods. Such a data base would be of immediate and direct use in pavement design and, with the corresponding soil and environmental data, could be also used to develop a general model of seasonal changes in resilient moduli of subgrade and base course soils.

The planned field investigations for validation of soil frost-susceptiblity tests provide an excellent opprotunity for collection of resilient modulus data on a number of subgrade soils and/or base courses of various types and properties. We propose to conduct both field and laboratory tests for that purpose.

A repeated-load plate bearing test is recommended for the field test. In this test repeated loads are applied to the test pavement through a circular plate or other loading medium and the recoverable, or resilient, deformation is recorded at the plate and on the adjacent pavement at set radial distances from the plate. The magnitude, frequency and wave-form of the cyclic loads are established to typify selected critical traffic conditions on highways or airfields. Resilient moduli of certain materials in the layered pavement system are determined by separate laboratory tests and are input, together with data from the plate-bearing tests, to a selected pavement response model to determine the resilient modulus of the subgrade or base course layer in question.

We have a project currently in progress at CRREL to obtain data in the manner outlined above. To date we have tested one silt and one clay subgrade soil Johnson et al. (1976) and have recently completed the first freeze-thaw cycle in tests on a silty sand. We have found it convenient to employ "full-depth," or all-bituminous-concrete (ABC) pavements, to minimize the number of layers in the system. Thus far, we have been able to use a 5-layer solution (CHEV-5L), although in some cases the system has required use of a larger modified Chevron program, which admits up to 15 layers. The BISTRO* program also has been used, and both the BISAR* program and a finite element model also are available and could be used if convenient.

The pavements selected for repeated-load plate bearing tests would be the same ones used for the frost-susceptibility validation testing mentioned above, which forms part of the same research project directed toward pavements in frost areas. For both types of tests it would be desirable to select test pavements at field sites having a wide range in subgrade soil types and moisture conditions. Also, for better effectiveness in achieving the objectives of both types of tests, it is desirable that the sites have simple pavement sections, since the complexity of multi-layered sections makes the acquisition of data on individual soils more difficult. In particular, it would be preferable that several sites have ABC pavements or pavements with only one type of base course material.

The instrumentation planned to be installed at the test sites for frost-susceptibility validation tests would be sufficient also for thaw-weakening. At each of the pavement sections selected for resilient modulus testing we propose to perform 6 to 10 loading tests during one calendar year for determination of the resilient modulus of the subgrade soil or base material.

The first loading test would be conducted when the sections were deeply frozen, followed by tests when thawing advanced into the layer in question about 5, 10, 20, and 40 cm. Further tests would be made when the soil profile had just reached a fully thawed state, and then after elapsed times of about 15, 30, 60 and 100-200 days. Depending on the conditions, certain of the tests might be omitted. When each test was performed, temperatures and moisture tension would be recorded by means of the installed thermocouples and tensiometers, and in some cases, a shallow boring would be made nearby to obtain moisture contents in the pavement section and subgrade. Prior to freezing and again when the sections were deeply frozen, special borings would be taken to obtain undisturbed cores of the base and subgrade materials and the bituminous concrete pavement for laboratory testing. The data from each plate bearing test would be analyzed, by means of the selected pavement response model, to calculate the resilient modulus of the base course or subgrade soil in question. The entire test series at each site, accordingly, would show the variation in modulus of that soil throughout a complete annual cycle. Of special interest are not only the absolute values of resilient moduli and their relationship with moisture content and moisture tension, but also the duration of the thaw-weakened condition and the rate of subsequent recovery.

It would also be useful to perform conventional static load testing at some of the test sites to determine the CBR and subgrade modulus (k, psi/in.) of the various materials. As these are destructive tests requiring excavation of pits to perform the tests on the surface of each layer, the tests probably would be feasible at only a few sites. Wherever such tests could be performed, it would be useful to compare the data with the resilient moduli determined by field and laboratory testing.

We propose to make use of the CRREL repeated-load plate bearing test device (a large semitrailer-mounted rig) at any sites located within a reasonable distance from Hanover, New Hampshire--possibly a radial distance of about 150 miles. At other sites it is hoped the FHWA test van might be made available, and at more distant sites other tests will be used, depending on the equipment available in the locality. One possibility is Dynaflect equipment or other similar devices, and the Benkelman beam could also be used. These devices are far from ideal, however, in the first case because of the low stress levels and in the second because of the low-speed, non-repetitive loading. Consequently, if no better alternatives are available, we would expect that at some sites it would be considered acceptable to forgo field loading tests and to determine the resilient properties of the materials exclusively by means of laboratory tests. In these cases the seasonal change of moisture content and moisture tension in the various layers of the pavement test section would be monitored to make it possible to relate the laboratory test moduli to specific times during the recovery process.

To obtain undisturbed core samples of unfrozen and frozen subgrade and base course materials it would be convenient to use CRREL drilling equipment, except at distant sites where equipment available in the locality would be used. In some pavement sections, we expect that it would prove impossible to obtain intact core samples of certain of the coarser-grained materials that may be poorly bonded even in the frozen state, due to a low ice content or to temperatures only slightly below freezing. In these cases loose samples would be taken,

*Courtesy Koninlijke/Shell Laboratorium - Amsterdam.

and remolded specimens would be prepared and frozen in the laboratory. If no better alternative is found, it may be decided in some cases to forgo laboratory resilient modulus testing and rely exclusively on field plate bearing tests for determination of seasonal variation in resilient moduli of the various materials.

The associated laboratory testing program would utilize a repeated load triaxial system. Subgrade and base course materials obtained from each test site in the frozen state would be subjected to controlled repeated triaxial loading in the frozen and thawed conditions to obtain resilient moduli and Poisson's ratios. In addition, undisturbed or remolded unfrozen samples would be tested to evaluate the range of seasonal conditions. Thawed samples would be tested over a range of moisture contents in order to simulate the recovery period. Attempts would be made to measure the prevailing stress state in the pore water before each series of repeated loads is applied.

Because the resilient modulus of an asphalt concrete pavement changes with temperature and moisture content, laboratory repeated-load tests would also be conducted at various environmental conditions on pavement cores obtained from the field sites. The applied load duration and frequency would duplicate that applied in the repeated-load plate bearing test. The tests would be conducted over a range of deviator and confining stress amplitudes to cover the range of stress levels anticipated at the test sites. The test results would be evaluated by statistical techniques, the product being the resilient modulus and Poisson's ratio as a function of the important variables. We expect that moisture tension would be a principal parameter in samples in which it can be successfully measured and continuously monitored. Other variables to be evaluated include the initial state (frozen, thawed, or never frozen), water content, density and the deviator and confining stress levels. The analysis selects the significant variables and provides coefficients necessary to calculate the seasonal values of the resilient modulus or Poisson's ratio. The results, thus determined, would be compared with the results obtained from the analysis of the repeated-load plate bearing tests on the field sections.

An attempt would also be made to develop a general model for the resilient modulus of the various elements of a pavement system. It is anticipated that this would be an empirical model based on observed relationships between the resilient modulus and parameters such as moisture tension, moisture content, density, temperature, permeability, time, confining stress, Poisson's ratio, and indices of material type. The success of the frost heave model would be dependent on the capability of this model to predict heave, and thus changes in moisture content and density under field conditions.

APPENDIX C: DERIVATION OF FINITE ELEMENT SYSTEM MATRICES

In this appendix, the solution of eq 41 is carried out term by term for the mth interior element. In this derivation x will be considered the local coordinate.

Let [s] be a 3 by 3 square matrix and be defined by the first two terms of eq 43 as follows and let <N> be defined as in the main text. In this derivation, eq 38 is expressed as:

$$k_1 \frac{\partial^2 u}{\partial x^2} + k_2 \frac{\partial u}{\partial x} = k_3 \frac{\partial u}{\partial t} + k_4$$

$$[s] = \int_0^{\ell} \left(k_1 \frac{\partial [N]^T}{\partial x} \frac{\partial [N]}{\partial x} + k_2 [N]^T \frac{\partial [N]}{\partial x} \right) dx$$

where $\langle N \rangle = \frac{1}{\ell^2} \left[(\ell^2 - 3\ell x + 2x^2),\ (4\ell x - 4x^2),\ (-\ell x + 2x^2) \right]$

$$s_{11} = \int_0^{\ell} \left[\frac{k_1}{\ell^4} (9\ell^2 - 24\ell x + 16x^2) + \frac{k_2}{\ell^4} (-3\ell^3 + 13\ell^2 x - 18\ell x^2 + 8x^3) \right] dx$$

$$= \frac{1}{\ell^4} \left[k_1 (9\ell^2 x - 12\ell x^2 + \frac{16x^3}{3} + k_2 (-3\ell^3 x + \frac{13\ell^2 x^2}{2} - 6\ell x^3 + 2x^4) \right]_0^{\ell}$$

$$= \frac{k_1}{\ell} (\frac{7}{3}) + k_2 (-\frac{1}{2})$$

$$s_{12} = \int_0^{\ell} \left[\frac{k_1}{\ell^4} (-12\ell^2 + 40\ell x - 32x^2) + \frac{k^2}{\ell^4} (4\ell^3 - 20\ell^2 x + 32\ell x^2 - 16x^3) \right] dx$$

$$= \frac{1}{\ell^4} \left[k_1 (-12\ell^2 x + 20\ell x^2 - \frac{32x^3}{3}) + k_2 (4\ell^3 x - 10\ell^2 x^2 + \frac{32\ell x^3}{3} - 4x^4) \right]_0^{\ell}$$

$$= \frac{k_1}{\ell} (-\frac{8}{3}) + k_2 (\frac{2}{3})$$

$$s_{13} = \int_0^{\ell} \left[\frac{k_1}{\ell^4} (3\ell^2 - 16\ell x + 16x^2) + \frac{k_2}{\ell^4} (-\ell^3 + 7\ell^2 x - 14\ell x^2 + 8x^3) \right] dx$$

$$= \frac{1}{\ell^4} \left[k_1 (3\ell^2 x - 8\ell x^2 + \frac{16x^2}{3}) + k_2 (-\ell^3 x + \frac{7\ell^2 x^2}{2} - \frac{14\ell x^3}{3} + 2x^4) \right]_0^{\ell}$$

$$= \frac{k_1}{\ell} (\frac{1}{3}) + k_2 (-\frac{1}{6})$$

$$s_{21} = \int_0^{\ell} \left[\frac{k_1}{\ell^4} (-12\ell^2 + 40\ell x - 32x^2) + \frac{k_2}{\ell^4} (-12\ell^2 x + 28\ell x^2 - 16x^3) \right] dx$$

$$= \frac{1}{\ell^4} \left[k_1 (-12\ell^2 x + 20\ell x^2 - \frac{32x^3}{3}) + k_2 (-6\ell^2 x^2 + \frac{28\ell x^3}{3} - 4x^4) \right]_0^{\ell}$$

$$= \frac{k_1}{\ell} (- \frac{8}{3}) + k_2 (- \frac{2}{3})$$

$$s_{22} = \int_0^{\ell} \left[\frac{k_1}{\ell^4} (16\ell^2 - 64\ell x + 64x^2) + \frac{k_2}{\ell^4} (16\ell^2 x - 48\ell x^2 + 32x^3) \right] dx$$

$$= \frac{1}{\ell^4} \left[k_1 (16\ell^2 x - 32\ell x^2 + \frac{64x^3}{3}) + k_2 (8\ell^2 x^2 - 16\ell x^3 + 8x^4) \right]_0^{\ell}$$

$$= \frac{k_1}{\ell} (\frac{16}{3}) + k_2 (0)$$

$$s_{23} = \int_0^{\ell} \left[\frac{k_1}{\ell^4} (-4\ell^2 + 24\ell x - 32x^2) + \frac{k_2}{\ell^4} \cdot (-4\ell^2 x + 20\ell x^2 - 16x^3) \right] dx$$

$$= \frac{1}{\ell^4} \left[k_1 (-4\ell^2 x + 12\ell x^2 - \frac{32x^3}{3}) + k_2 (-2\ell^2 x^2 + \frac{20\ell x^3}{3} - 4x^4) \right]_0^{\ell}$$

$$= \frac{k_1}{\ell} (- \frac{8}{3}) + k_2 (\frac{2}{3})$$

$$s_{31} = \int_0^{\ell} \left[\frac{k_1}{\ell^4} (3\ell^2 - 16\ell x + 16x^2) + \frac{k_2}{\ell^4} (3\ell^2 x - 10\ell x^2 + 8x^3) \right] dx$$

$$= \frac{1}{\ell^4} \left[k_1 (3\ell^2 x - 8\ell x^2 + \frac{16x^3}{3}) + k_2 (\frac{3\ell^2 x^2}{2} - \frac{10\ell x^3}{3} + 2x^4) \right]_0^{\ell}$$

$$= \frac{k_1}{\ell} (\frac{1}{3}) + k_2 (\frac{1}{6})$$

$$s_{32} = \int_0^{\ell} \left[\frac{k_1}{\ell^4} (-4\ell^2 + 24\ell x - 32x^2) + \frac{k_2}{\ell^4} (-4\ell^2 x + 16\ell x^2 - 16x^3) \right] dx$$

$$= \frac{1}{\ell^4}\left[k_1\left(-4\ell^2x + 12\ell x^2 - \frac{32x^3}{3}\right) + k_2\left(-2\ell x^2 + \frac{16\ell x^3}{3} - 4x^4\right)\right]_0^{\ell}$$

$$= \frac{k_1}{\ell}\left(-\frac{8}{3}\right) + k_2\left(-\frac{2}{3}\right)$$

$$s_{33} = \int_0^{\ell}\left[\frac{k_1}{\ell^4}\left(\ell^2 - 8\ell x + 16x^2\right) + \frac{k_2}{\ell^4}\left(\ell^2 x - 6\ell x^2 + 8x^3\right)\right] dx$$

$$= \frac{1}{\ell^4}\left[k_1\left(\ell^2 x - 4\ell x^2 + \frac{16x^3}{3}\right) + k_2\left(\frac{\ell^2 x^2}{2} - 2\ell x^3 + 2x^4\right)\right]_0^{\ell}$$

$$= \frac{k_1}{\ell}\left(\frac{7}{3}\right) + k_2\left(\frac{1}{2}\right)$$

Let [p] be a 3 by 3 square matrix, <N> be defined as previously and let [p] equal the third term in eq 43 as follows:

$$[p] = \int_0^{\ell} k_3 (N)^T (N)\, dx$$

$$p_{11} = \int_0^{\ell} \frac{1}{\ell^4} k_3\left(\ell^4 - 6\ell^3 x + 13\ell^2 x^2 - 12\ell x^3 + 4x^4\right) dx$$

$$= \frac{k_3}{\ell^4}\left[\ell^4 x - 3\ell^3 x^2 + \frac{13\ell^2 x^3}{3} - 3\ell x^4 + \frac{4x^5}{5}\right]_0^{\ell}$$

$$= k_3\ell\left(\frac{2}{15}\right)$$

$$p_{12} = \int_0^{\ell} \frac{1}{\ell^4} k_3\left(4\ell^3 x - 16\ell^2 x^2 + 20\ell x^3 - 8x^4\right) dx$$

$$= \frac{k_3}{\ell^4}\left[2\ell^3 x^2 - \frac{16\ell^2 x^3}{3} + 5\ell x^4 - \frac{8x^5}{5}\right]_0^{\ell}$$

$$= k_3\ell\left(\frac{1}{15}\right)$$

$$p_{13} = \int_0^{\ell} \frac{k_3}{\ell^4} (-\ell^3 x + 5\ell^2 x^2 - 8\ell x^3 + 4x^4)\, dx$$

$$= \frac{k_3}{\ell^4} \left[-\frac{\ell^3 x^2}{2} + \frac{5\ell^2 x^3}{3} - 2\ell x^4 + \frac{4x^5}{5} \right]_0^{\ell}$$

$$= k_3 \ell \left(-\frac{1}{30} \right)$$

$$p_{21} = p_{12} = k_3 \ell \left(\frac{1}{15} \right)$$

$$p_{22} = \int_0^{\ell} \frac{k_3}{\ell^4} (16\ell^2 x^2 - 32\ell x^3 + 16x^4)\, dx$$

$$= \frac{k_3}{\ell^4} \left[\frac{16\ell^2 x^3}{3} - 8\ell x^4 + \frac{16x^5}{5} \right]_0^{\ell}$$

$$= k_3 \ell \left(\frac{8}{15} \right)$$

$$p_{23} = \int_0^{\ell} \frac{k_3}{\ell^4} (-4\ell^2 x^2 + 12\ell x^3 - 8x^4)\, dx$$

$$= \frac{k_3}{\ell^4} \left[\frac{-4\ell^2 x^3}{3} + 3\ell x^4 - \frac{8x^5}{5} \right]_0^{\ell}$$

$$= k_3 \ell \left(\frac{1}{15} \right)$$

$$p_{31} = p_{13} = k_3 \ell \left(-\frac{1}{30} \right)$$

$$p_{32} = p_{23} = k_3 \ell \left(\frac{1}{15} \right)$$

$$p_{33} = \int_0^{\ell} \frac{k_3}{\ell^4} \ell^2 x^2 - 4\ell x^3 + 4x^4)\, dx$$

$$= \frac{k_3}{\ell^4} \left[\frac{\ell^2 x^3}{3} - \ell x^4 + \frac{4x^5}{5} \right]_0^{\ell}$$

$$= k_3 \ell \left(\frac{2}{15} \right)$$

Let {f} be a column matrix, and let <N> be defined as previously given, and let {f} equal the last term in eq 43 modified as follows:

$$\{f\} = \int_0^{\ell} k_4 (N)^T \, dx$$

$$f_1 = \int_0^{\ell} \frac{k_4}{\ell^2} (\ell^2 - 3\ell x + 2x^2) \, dx$$

$$= \frac{k_4}{\ell^2} \left[\ell^2 x - \frac{3\ell x^2}{2} + \frac{2x^3}{3} \right]_0^{\ell}$$

$$= k_4 \ell \left(\frac{1}{6} \right)$$

$$f_2 = \int_0^{\ell} \frac{k_4}{\ell^2} (4\ell x - 4x^2) \, dx$$

$$= \frac{k_4}{\ell^2} \left[2\ell x^2 - \frac{4x^3}{3} \right]_0^{\ell}$$

$$= k_4 \ell \left(\frac{2}{3} \right)$$

$$f_3 = \int_0^{\ell} \frac{k_4}{\ell^2} (-\ell x + 2x^2) \, dx$$

$$= \frac{k_4}{\ell^2} \left[-\frac{\ell x^2}{2} + \frac{2x^3}{3} \right]_0^{\ell}$$

$$= k_4 \ell \left(\frac{1}{6} \right)$$

Finally, assembling all the above into standard matrix notation

$$[s] = \frac{k_1}{3\ell} \begin{bmatrix} 7 & -8 & 1 \\ -8 & 16 & -8 \\ 1 & -8 & 7 \end{bmatrix} + \frac{k_2}{6} \begin{bmatrix} -3 & 4 & -1 \\ -4 & 0 & 4 \\ 1 & -4 & 3 \end{bmatrix}$$

$$[p] = \frac{k_3 \ell}{30} \begin{bmatrix} 4 & 2 & -1 \\ 2 & 16 & 2 \\ -1 & 2 & 4 \end{bmatrix}$$

$$\{f\} = \frac{k_4 \ell}{6} \begin{Bmatrix} 1 \\ 4 \\ 1 \end{Bmatrix}$$

These equations are the element system equation in

$$[s]\{u\} + [p]\{u\} = \{f\}$$

which is the finite element solution of eq 43 modified for the spatial domain only. The temporal solution is by the Crank-Nicholson method and was discussed in the text. The following section presents an assemblage of the M element matrices into the solution scheme for the entire solution domain.

Assembly of system matrices

The global system matrices are obtained by appropriately assembling the element solutions obtained before. After assemblage the result may be generalized as follows:

$$[S]\{u\} + [P]\{\dot{u}\} = \{F\}$$

where [S] is a square banded nonsymmetrical matrix because of the k_2 term in [s], [P] is a square banded symmetric matrix and {F} is a column matrix. The matrices are functions of the k_i parameters and geometrical discretion of the system and are known. The unknown matrices are u and $\{\dot{u}\}$ which are the nodal values of the state variable for each node of the problem. Recall that the dot (in $\{\dot{u}\}$) refers to the time derivative.

The system matrices are as follows before considering the boundary conditions:

$$[S] = \begin{bmatrix}
s^1_{11} & s^1_{12} & s^1_{13} & & & & & & & & \\
s^1_{21} & s^1_{22} & s^1_{23} & & & & & & & & \\
s^1_{31} & s^1_{32} & s^1_{33}+s^2_{11} & s^2_{12} & s^2_{13} & & & & & & \\
 & & s^2_{21} & s^2_{22} & s^2_{23} & & & & & & \\
 & & s^2_{31} & s^2_{32} & s^2_{33}+s^3_{11} & & & & & & \\
 & & & & & \ddots & & & & & \\
 & & & & & & \ddots & & & & \\
 & & & & & & & \ddots & & & \\
 & & & & & & & s^{m-1}_{33}+s^m_{11} & s^m_{12} & s^m_{13} \\
 & & & & & & & s^m_{21} & s^m_{22} & s^m_{23} \\
 & & & & & & & s^m_{31} & s^m_{32} & s^m_{33}
\end{bmatrix}$$

[P] is identically formed, and

$$\{F\} = \begin{bmatrix} f_1^1 \\ f_2^1 \\ f_3^1 + f_1^2 \\ f_2^2 \\ f_3^2 + f_1^3 \\ \vdots \\ f_3^{m-1} + f_1^m \\ f_2^m \\ f_3^m \end{bmatrix}$$

The superscript refers to the element number and the subscript refers to the values position in the element system matrices.

Considering specified boundary conditions at the ends of the solution domain, $u_{x=0} = u_u$ and $u_{x=L} = u_L$, the above matrices became

$$[S] = \begin{bmatrix} 1 & 0 & 0 & & & & & & & & & \\ 0 & s_{22}^1 & s_{23}^1 & & & & & & & & & \\ 0 & s_{32}^1 & s_{33}^1 + s_{11}^2 & s_{12}^2 & s_{13}^2 & & & & & & & \\ & & s_{21}^2 & s_{22}^2 & s_{23}^2 & & & & & & & \\ & & s_{31}^2 & s_{32}^2 & s_{33}^2 + s_{11}^3 & & & & & & & \\ & & & & & \ddots & & & & & & \\ & & & & & & \ddots & & & & & \\ & & & & & & & \ddots & & & & \\ & & & & & & & & s_{33}^{m-1} + s_{11}^m & s_{12}^m & 0 \\ & & & & & & & & s_{21}^m & s_{22}^m & 0 \\ & & & & & & & & 0 & 0 & 1 \end{bmatrix}$$

$$[P] = \begin{bmatrix} 0 & 0 & 0 & & & & & & & & \\ 0 & p^1_{22} & p^1_{23} & & & & & & & & \\ 0 & p^1_{32} & p^1_{33} + p^2_{11} & p^2_{12} & p^3_{13} & & & & & & \\ & & p^2_{21} & p^2_{22} & p^2_{23} & & & & & & \\ & & p^2_{31} & p^2_{32} & p^2_{33} & p^3_{11} & & & & & \\ & & & & & \bullet & & & & & \\ & & & & & & \bullet & & & & \\ & & & & & & & \bullet & & & \\ & & & & & & & & p^{m-1}_{33} + p^m_{11} & p^m_{12} & 0 \\ & & & & & & & & p^m_{21} & p^m_{22} & 0 \\ & & & & & & & & 0 & 0 & 0 \end{bmatrix}$$

and

$$\{F\} = \begin{Bmatrix} u_u \\ f^1_2 - u_u s^1_{21} \\ f^1_3 + f^2_1 - u_u s^1_{31} \\ f^2_2 \\ \cdot \\ \cdot \\ \cdot \\ f^{m-1}_3 + f^m_1 - u_L s^m_{13} \\ f_2 - u_L s^m_{23} \\ u_L \end{Bmatrix}$$

If a boundary is assumed to be a natural boundary, i.e. $\partial u/\partial x = 0$, modification of the system matrices is not required. For instance, assume that at $x = 0$ there is a natural boundary condition, then the first part of the system matrices would be the same as the first unmodified matrices above.

A second order polynomial (quadratic) shape function was used to develop the finite-element analog. Other shape functions are also possible. Previous work, Guymon (1976), contained a derivation of the element systems matrices for a linear shape function. The use of a second order shape function requires more core storage for computer solution; however, accuracy has been improved.

Computer storage of arrays

A substantial benefit of the finite-element method is that the system matrices are "naturally" banded. Consequently, computer storage arrays can be substantially reduced if only the nonzero information in the arrays is stored. This is accomplished as is illustrated in the following figure:

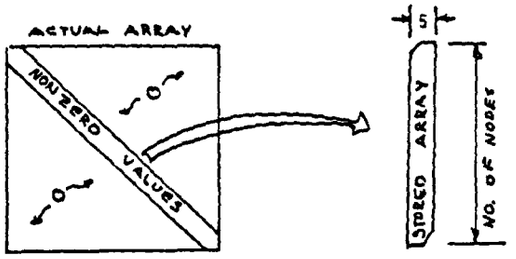

Thus, if the number of nodes in a problem is N, the required storage for the [S] array is N by 5. If the entire array were stored, the storage required would be N by N. Algorithms are specially coded to accommodate the banded storage concept which also saves substantial computer execution time since operations with zeros are not carried out.

A facsimile catalog card in Library of Congress MARC format is reproduced below.

Berg, R.L.
Mathematical model to correlate frost heave of pavements with laboratory predictions / by R.L. Berg, G.L. Guymon and T.C. Johnson. Hanover, N.H.: U.S. Cold Regions Research and Engineering Laboratory; Springfield, VA.: available from National Technical Information Service, 1980.
vi, 54 p., illus.; 27 cm. (CRREL Report 80-10.)
Prepared for Federal Aviation Administration, Federal Highway Administration, U.S. Army Corps of Engineers, Office, Chief of Engineers by Corps of Engineers, U.S. Army Cold Regions Research and Engineering Laboratory, under DA Project 4A762730AT42.
Bibliography: p. 29.
1. Computerized simulation. 2. Frost heave. 3. Laboratory tests. 4. Mathematical models. 5. Pavements. 6. Soil tests. I. United States. Army. Corps of Engineers. II. Army Cold Regions Research and Engineering Laboratory, Hanover, N.H. III. Series: CRREL Report 80-10.